

# *Toward Better Understanding of Sprite Streamers: Initiation, Morphology, and Polarity Asymmetry*

**Victor P. Pasko, Jianqi Qin & Sebastien Celestin**

## **Surveys in Geophysics**

An International Review Journal  
Covering the Entire Field of Geosciences  
and Related Areas

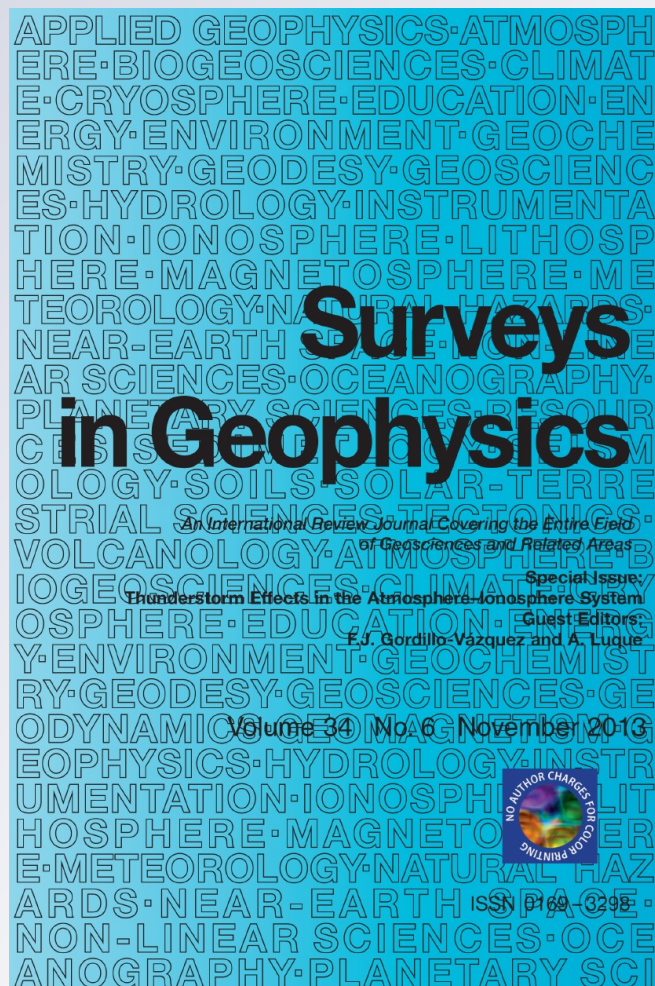
ISSN 0169-3298

Volume 34

Number 6

Surv Geophys (2013) 34:797-830

DOI 10.1007/s10712-013-9246-y



**Your article is protected by copyright and all rights are held exclusively by Springer Science +Business Media Dordrecht. This e-offprint is for personal use only and shall not be self-archived in electronic repositories. If you wish to self-archive your article, please use the accepted manuscript version for posting on your own website. You may further deposit the accepted manuscript version in any repository, provided it is only made publicly available 12 months after official publication or later and provided acknowledgement is given to the original source of publication and a link is inserted to the published article on Springer's website. The link must be accompanied by the following text: "The final publication is available at [link.springer.com](http://link.springer.com)".**

# Toward Better Understanding of Sprite Streamers: Initiation, Morphology, and Polarity Asymmetry

Victor P. Pasko · Jianqi Qin · Sebastien Celestin

Received: 12 November 2012 / Accepted: 21 June 2013 / Published online: 12 July 2013  
© Springer Science+Business Media Dordrecht 2013

**Abstract** This paper presents a literature survey on the recent developments related to modeling studies of transient luminous events termed sprites and sprite halos that are produced at mesospheric and lower ionospheric altitudes in the Earth's atmosphere by lightning. The primary emphasis is placed on publications that appeared in the refereed literature starting from year 2010 and up to the present date. The survey focuses on the interpretation of morphological features observed in sprites. We introduce parameters typically used for quantitative description of electron avalanches and discuss the importance of space charge effects on different spatial scales, including sprite halos (exhibiting 10s of km transverse extents) and sprite streamers (requiring submeter resolution for accurate description). A special emphasis is placed on the interpretation of initiation and development of sprite streamers captured in high-speed video observations and a critical review of the most recent modeling efforts related to these observations. We also discuss fundamental reasons for polarity asymmetry in existing sprite observations indicating that vast majority of sprites with well-developed streamer structure are produced by positive cloud-to-ground lightning discharges.

**Keywords** Atmospheric electricity · Lightning · Sprites · Sprite halos · Sprite streamers

---

V. P. Pasko (✉)

Communications and Space Sciences Laboratory (CSSL), Department of Electrical Engineering,  
The Pennsylvania State University, 211B Electrical Engineering East, University Park,  
PA 16802-2706, USA  
e-mail: vpasko@psu.edu

J. Qin

Communications and Space Sciences Laboratory (CSSL), Department of Electrical Engineering,  
The Pennsylvania State University, 227 Electrical Engineering East, University Park,  
PA 16802-2706, USA  
e-mail: juq108@psu.edu

S. Celestin

Laboratory of Physics and Chemistry of the Environment and Space (LPC2E), CNRS,  
University of Orleans, 3A Avenue de la Recherche Scientifique, 45071 Orleans Cedex 2, France  
e-mail: sebastien.celestin@cnrs-orleans.fr

## 1 Introduction

Sprites are large-scale transient luminous events that are produced at altitudes  $\sim 40\text{--}90$  km by lightning discharges (Sentman et al. 1995; Lyons 1996). They typically develop at the base of the ionosphere and move rapidly downwards at speeds up to 10,000 km/s (Stanley et al. 1999; Gerken et al. 2000; Cummer et al. 2006; McHarg et al. 2007; Stenbaek-Nielsen et al. 2007; Stenbaek-Nielsen and McHarg 2008). Sprites consist of a large number of vertically oriented filamentary plasma structures referred to as sprite streamers (e.g., McHarg et al. 2011, and references therein). Sprite halos, or simply halos, are brief descending glows with lateral extent 40–70 km and upwardly concave shape, which sometimes (but not always) are observed to accompany or precede more structured sprites (Barrington-Leigh et al. 2001; Frey et al. 2007).

The experimental and theoretical findings related to sprites and other types of transient luminous events have been summarized in several extensive review articles (Boeck et al. 1998; Rodger 1999; Inan 2002; Inan et al. 2010; Lyons et al. 2003; Pasko 2006, 2007, 2008, 2010; Raizer et al. 2010; Neubert et al. 2008; Roussel-Dupre et al. 2008; Mishin and Milikh 2008; Ebert and Sentman 2008; Ebert et al. 2010; Siingh et al. 2008; Pasko et al. 2012; Kuo 2012; Surkov and Hayakawa 2012). The goal of the present paper is to focus on the most recent progress in understanding of observed morphological features of sprite streamers, emphasizing refereed literature that appeared starting from 2010 and up to the present date. Morphological features of sprite streamers as documented in recent high-speed video observations have been summarized in an accompanying Surveys in Geophysics paper (Stenbaek-Nielsen et al. 2013) and readers are referred to that document, in particular, for the description of extensive experimental evidence related to column and carrot sprites.

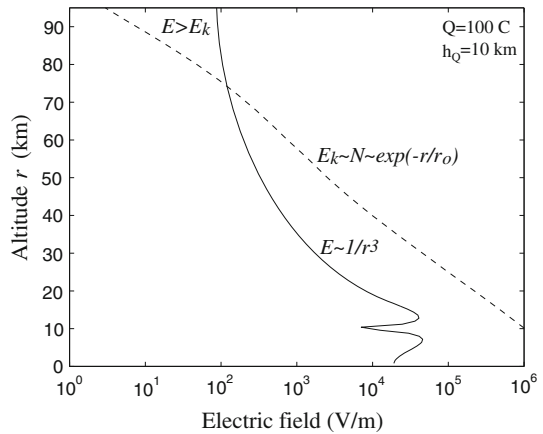
## 2 Physical Mechanism of Sprites

In this section, we review some background information relevant to sprite streamers and sprite halos.

### 2.1 Large-Scale Electrodynamics

The possibility of large-scale gas discharge events above thunderclouds, which we currently know as sprite phenomenon, was first predicted in 1925 by the Nobel Prize winner Wilson (1925). He first recognized that the relationship between the thundercloud electric field, which decreases with altitude  $r$  (Fig. 1) as  $\sim r^{-3}$ , and the critical breakdown field  $E_k$ , which falls more rapidly (being proportional to the exponentially decreasing air density  $N$ ) leads to the result that “there will be a height above which the electric force due to the cloud exceeds the sparking limit” (Wilson 1925). Here, and in subsequent parts of this paper,  $E_k$  is used to denote the conventional breakdown threshold field defined by the equality of the ionization and dissociative attachment coefficients in air (Raizer 1991, p. 135). The recent studies commonly employ a model value  $E_k \simeq 2.87 \times 10^6$  V/m at atmospheric pressure (Morrow and Lowke 1997). It should be noted that due to the finite atmospheric conductivity above thunderclouds, the dipole field configuration shown in Fig. 1 is realized at mesospheric altitudes only during very transient time periods  $\sim 1\text{--}10$  ms following intense lightning discharges, in part defining a similarly transient nature of the observed sprite phenomenon (Pasko et al. 1997, and references cited therein).

**Fig. 1** Physical mechanism of sprites (Wilson 1925): “while the electric force due to the thundercloud falls off rapidly as  $r$  increases, the electric force required to causing sparking (which for a given composition of the air is proportional to its density) falls off still more rapidly. Thus, if the electric moment of a cloud is not too small, there will be a height above which the electric force due to the cloud exceeds the sparking limit.”



The mechanism of the penetration of the thundercloud electric fields to the higher-altitude regions is illustrated in Fig. 2. As the thundercloud charges slowly build up before a lightning discharge, high-altitude regions are shielded from the quasi-electrostatic fields of the thundercloud charges by the space charge induced in the conducting atmosphere at the lower altitudes. The appearance of this shielding charge is a consequence of the finite vertical conductivity gradient of the atmosphere above the thundercloud. When one of the thundercloud charges (e.g., the positive one as shown in Fig. 2) is quickly removed by a lightning discharge, the remaining shielding charges of opposite sign produce a large quasi-electrostatic field that appears at all altitudes above the thundercloud and endures for a time equal to approximately (see related discussion in Pasko et al. 1997) the local relaxation time ( $\tau_\sigma = \epsilon_0/\sigma$ , where  $\sigma$  is the local conductivity and  $\epsilon_0$  is the permittivity of free space) at each altitude. These temporarily existing electric fields lead to the heating of ambient electrons and the generation of ionization changes and optical emissions known as sprite phenomenon.

Figure 3 illustrates the above-discussed scenario by showing model calculations of the vertical component of the electric field at altitudes 50, 60, 70, and 80 km directly above a positive lightning discharge removing 200 C of charge from altitude 10 km in 1 ms (Pasko et al. 1997). During a very transient time period  $\sim 1$  ms, mostly defined by atmospheric conductivity profile, the electric field can reach values on the order of the critical breakdown threshold field  $E_k$  at mesospheric/lower ionospheric altitudes. The quasi-static approximation employed here is valid for relatively slow source variations with timescales  $>0.5$  ms (Pasko et al. 1999).

It should be emphasized that the simplified schematics shown in Fig. 2 is employed to discuss the physical concept of penetration of large electric field transients to mesospheric altitudes and by no means reflects the complexity of charge distributions observed in thunderclouds. In cases of more realistic charge distributions in the thundercloud, which sometimes involve up to six charge layers in the vertical direction (Marshall and Rust 1993; Shepherd et al. 1996), each of the charge centers can be viewed as generating its own polarization charge in and above the thundercloud, and the resultant configuration of the electric field and charge density can be obtained by using the principle of superposition. This consideration is helpful in visualization of the fact that the electric field appearing at mesospheric altitudes after the charge removal by a cloud-to-ground lightning discharge is defined mostly by the absolute value  $Q$  and altitude  $h_Q$  of the removed charge and is

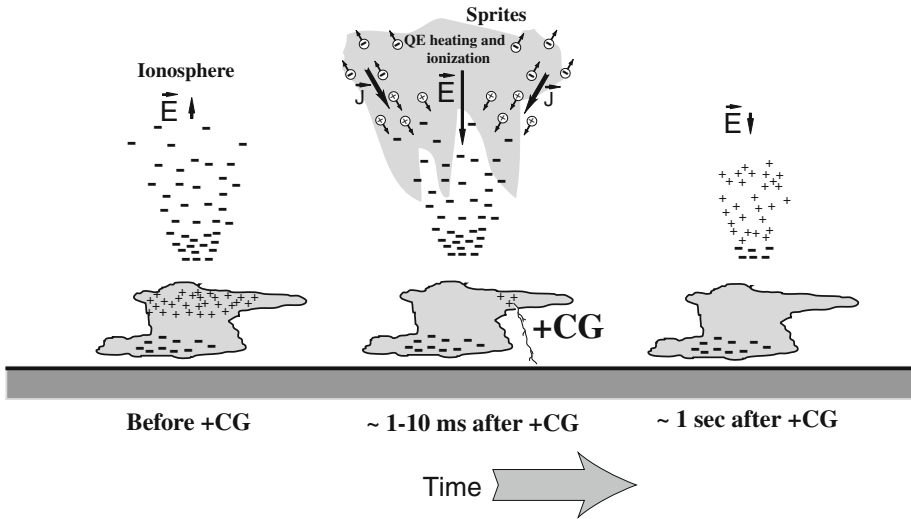
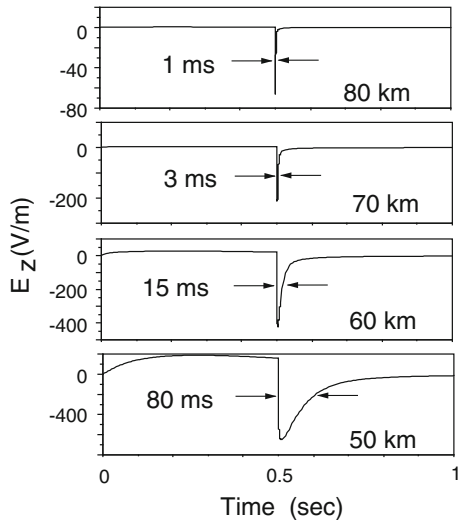


**Fig. 2** Illustration of the mechanism of penetration of large electric fields to mesospheric altitudes following a positive cloud-to-ground (+CG) lightning discharge (Pasko et al. 1997). Reprinted by permission from American Geophysical Union

**Fig. 3** Time dynamics of the vertical component of the electric field at selected altitudes directly above a positive cloud-to-ground lightning discharge (Pasko et al. 1997). Reprinted by permission from American Geophysical Union



essentially independent of the complexity of the charge configuration in the cloud. The charge removal can also be viewed as the “placement” of an identical charge of opposite sign. The initial field above the cloud is simply the free space field due to the “newly placed” charge and its image in the ground, which is assumed to be perfectly conducting.

The charge moment change  $Qh_Q$  (i.e., charge removed by lightning  $Q$  times the altitude from which it was removed  $h_Q$  mentioned above) represents the key parameter that is used in sprite literature to measure the strength of lightning in terms of sprite production potential (e.g., Lang et al. 2011, and references therein). In spite of the apparent simplicity of the basic mechanism of penetration of large quasi-electrostatic fields to the mesospheric

altitudes described above and depicted in Fig. 2, the observed sprite morphology and time dynamics appear to be quite complex. In terms of general gas discharge theory (Raizer 1991; Pasko 2006), the sprite situation corresponds to relatively large  $pd$  values, where  $p$  is the gas pressure and  $d$  is effective discharge gap length, fully sufficient for the development of streamers. The sprite discharges are therefore expected to proceed in the form of streamers. Some additional corrections are required to account for relatively dense plasma at the lower ledge of the Earth's ionosphere at altitudes 80–90 km where diffuse optical emissions of sprite halos are sometimes observed. Basic properties of both sprite streamers and sprite halos are introduced in the next subsection.

## 2.2 Vertical Structuring of Sprites

Pasko et al. (1998a) proposed a theory indicating that sprite structure as a function of altitude should exhibit a transition from essentially nonstructured diffuse glow at altitudes  $\geq 85$  km to the highly structured streamer region at altitudes  $\leq 75$  km (Fig. 4). It was proposed that the vertical structuring in sprites is created due to interplay of three physical timescales: (1) The dissociative attachment timescale  $\tau_a$  (which is defined by the maximum net attachment frequency as  $1/(v_a - v_i)_{\max}$ , where  $v_i$  and  $v_a$  are the ionization and attachment frequencies, respectively); (2) The ambient dielectric relaxation timescale  $\tau_\sigma = \epsilon_0/\sigma$ ; (3) The timescale for the development of an individual electron avalanche into a streamer  $t_s$  (this is an effective time over which the electron avalanche generates a space charge field comparable in magnitude to the externally applied field (Pasko et al. 1998a)). The persistence of the electric field at lower altitudes on timescales  $\tau$  exceeding those required for the initiation of streamers ( $\tau > t_s$ ) is the basic reason for the appearance of streamers, while the diffuse glow is predominant at higher altitudes ( $\tau < t_s$ ). The most recent work indicates the importance of electron detachment and existence of relatively large plasma inhomogeneities in the lower ionosphere to facilitate the initiation of sprite streamers with observed values of lightning charge moment changes. These most recent results will be discussed in Sect. 3. In view of the importance of accurate representation of the avalanche-to-streamer transition for understanding of the initiation of sprite streamers, we also include a separate discussion on this concept as part of introduction in Sect. 2.4.

Barrington-Leigh et al. (2001) conducted one-to-one comparison between high-speed video observations of sprites and a fully electromagnetic model of sprite-driving fields and optical emissions. Sprite halos are brief descending glows with lateral extent 40–70 km, which sometimes observed to accompany or precede more structured sprites. The analysis conducted in Barrington-Leigh et al. (2001) demonstrated a very close agreement of model optical emissions and high-speed video observations, and for the first time identified sprite halos as being produced entirely by quasi-electrostatic thundercloud fields. Sprites indeed often exhibit sprite halos that appear as relatively amorphous nonstructured glow at sprite tops and that convert to highly structured, streamer-dominated regions at lower altitudes (e.g., Stanley et al. 1999; Gerken et al. 2000, and references therein). This vertical structure in sprites is apparent in many existing high-speed video observations and can be clearly seen in Fig. 4b.

Sprite halos and sprite streamers are closely interlinked phenomena as both are driven by quasi-static electric fields produced by lightning. The optical manifestation of these phenomena depends on magnitude and time dynamics of the charge moment change and lower ionospheric conditions (i.e., electron density profile and presence of inhomogeneities). When the diffuse glow of sprite halo is the only visible emission, it does not mean that sprite streamers are not present in the same volume as they usually require additional

exponential growth to become visible (see discussion in Sect. 2.3 below). Similarly, when only sprite streamers are observed optically, the diffuse sprite halo emissions may remain subvisual (Qin et al. 2013). The observability of sprite streamers and halos depends on the specifics of the observational instruments used and the distance. It is therefore not appropriate to describe sprite streamers with no visible halo emissions as “pure sprites” or halos with no visible streamer structures as “pure halos” in observations.

### 2.3 Basic Properties of Sprite Streamers and Similarity Relations

Streamers mentioned in the previous section can be defined as narrow filamentary plasmas, which are driven by highly nonlinear space charge waves (Raizer 1991, p. 327). At ground level, the streamer has a radius of  $10^{-1}$ – $10^{-2}$  cm and propagates with a velocity of  $10^5$ – $10^7$  m/s. The dynamics of a streamer is mostly controlled by a highly enhanced field region, known as a streamer head. A large amount of net space charge exists in the streamer head, which strongly enhances the electric field in the region just ahead of the streamer, while screening the ambient field out of the streamer channel. The peak space charge field can reach a value many times the  $E_k$  threshold. The large space charge field leads to a very intense electron impact ionization occurring in the streamer head. This ionization rapidly raises electron density from an ambient value to the level in the streamer channel, resulting in the spatial extension of the streamer. The streamer polarity is defined by a sign of the charge in its head. The positive streamer propagates against the direction of the electron drift and requires ambient seed electrons avalanching toward the streamer head for the spatial advancement (Dhali and Williams 1987). The negative streamer is generally able to propagate without the seed electrons since electron avalanches originating from the streamer head propagate in the same direction as the streamer (Vitello et al. 1994; Rocco

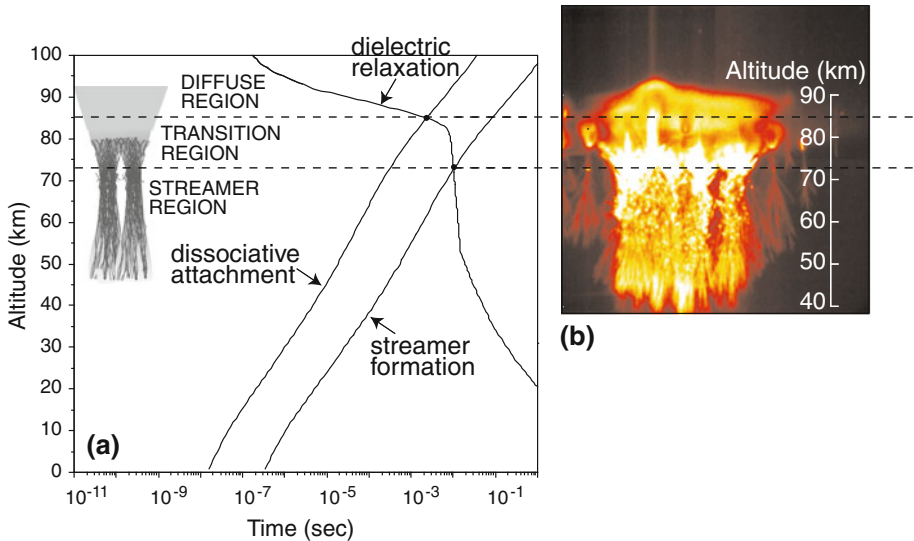


**Fig. 4** The vertical altitude structuring of optical emissions in sprites. **a** The altitude distribution of different timescales characterizing the vertical structuring of optical emissions in sprites (Pasko et al. 1998a; Pasko and Stenbaek-Nielsen 2002). **b** Results of video observations (Stenbaek-Nielsen et al. 2000). Reprinted by permission from American Geophysical Union

et al. 2002). The minimum field required for the propagation of positive streamers in air at ground pressure has been extensively documented experimentally and usually stays close to the value  $E_{cr}^+ = 4.4$  kV/cm (Allen and Ghaffar 1995), in agreement with the results of numerical simulations of positive streamers (Babaeva and Naidis 1997; Morrow and Lowke 1997). The absolute value of the similar field  $E_{cr}^-$  for negative streamers is a factor of 2–3 higher (Babaeva and Naidis 1997; Raizer 1991, p. 136). One of the estimates of this field is  $E_{cr}^- = 12.5$  kV/cm, in accordance with Fig. 7 in (Babaeva and Naidis 1997). The value  $E_{cr}^- \simeq 12.5$  kV/cm is not well established, and different sources list various values ranging from 7.5 kV/cm (Gallimberti et al. 2002) to 10 kV/cm (Bazelyan and Raizer 2000, p. 198). The fields  $E_{cr}^+$  and  $E_{cr}^-$  are the minimum fields needed for the propagation of individual positive and negative streamers, but not for their initiation (Petrov and Petrova 1999). Streamers can be launched by individual electron avalanches in large fields exceeding the  $E_k$  threshold, or by initial sharp points creating localized field enhancements, which is a typical case for point-to-plane discharge geometries (Raizer et al. 1998; Briels et al. 2006). The possibility of simultaneous launching (in opposite directions) of positive and negative streamers from a single midgap electron avalanche is documented experimentally (Loeb and Meek 1940; Raizer 1991, p. 335) and reproduced in numerical experiments (Vitello et al. 1993; Liu and Pasko 2004; Bourdon et al. 2007).

The above-mentioned values of  $E_k$ ,  $E_{cr}^+$ , and  $E_{cr}^-$  correspond to ground pressure. It is commonly assumed in sprite studies that these fields can be directly scaled proportionally to atmospheric neutral density  $N$  to find corresponding values at sprite altitudes. This approach is generally justified by similarity laws (Pasko 2006). We note, however, that the actual scaling of  $E_{cr}^+$  and  $E_{cr}^-$  for the sprite altitude range has not yet been verified experimentally.

Similarity laws mentioned above (Roth 1995; Liu and Pasko 2006, and references therein) represent a useful tool for the analysis of gas discharges since they allow to use known properties of the discharge at one pressure to deduce features of discharges at variety of other pressures of interest, at which experimental studies may not be feasible or even possible. Similarity laws for streamers propagating in nonuniform gaps in air at high (i.e., several atmospheric) pressures have been studied in (Tardiveau et al. 2001; Achat et al. 1992). The similarity properties of streamers at different air pressures are also of great interest for the interpretation of morphology observed in high-altitude sprite discharges (Pasko et al. 1998a; Liu and Pasko 2004).

Figure 5 illustrates similarity scaling of streamers using results of model calculations of electron densities corresponding to double-headed streamers developing at altitudes 0, 30, and 70 km in electric field  $E_0 = 1.5E_k$ . In accordance with the similarity relationships, the streamer timescales, the streamer spatial scales, and the streamer electron densities scale with the air density as  $\sim 1/N$ ,  $\sim 1/N$ , and  $\sim N^2$ , respectively, and the scaled streamer characteristics remain otherwise identical for the same values of the reduced electric field  $E/N$  (Pasko et al. 1998a). In order to facilitate the discussion of similarity properties of streamers at different altitudes/air densities, the results presented in Fig. 5b, c are given at the moments of time, which are obtained by scaling ( $\sim 1/N$ ) of the ground value, 2.7 ns, specified in Fig. 5a. The horizontal and vertical dimensions of the simulation boxes in Fig. 5b, c also directly correspond to scaled ( $\sim 1/N$ ) ground values shown in Fig. 5a. The electron density scale in Fig. 5b, c also corresponds to scaled ( $\sim N^2$ ) values given in Fig. 5a. The differences observed between model streamers at the ground and at 30 and 70 km altitudes in Fig. 5 are primarily due to the reduction in photoelectron production at high atmospheric pressures through the quenching of UV emitting excited states of  $N_2$  (Liu and Pasko 2004). In all shown cases, model streamers exhibit fast acceleration and

expansion (Liu and Pasko 2004). The fast expansion and acceleration are fundamental properties of streamers that will be discussed in Sect. 3 in the context of the most recent high-speed video observations of sprites.

It is important to emphasize that the effective streamer diameters observed by an imager focusing on sprite structures at different altitudes would inevitably depend on the geometry of the mesospheric electric fields and the history of the sprite development (i.e., the altitude of the initiation point(s)). Gerken et al. (2000) and Gerken and Inan (2002, 2003) employed a telescopic imager to measure effective streamer diameters at different altitudes in sprites. The measured diameters are 60–145 m ( $\pm 12$  m), 150 m ( $\pm 13$  m), 196 m ( $\pm 13$  m), for altitude ranges 60–64 km ( $\pm 4.5$  km), 76–80 km ( $\pm 5$  km), 81–85 km ( $\pm 6$  km), respectively. Although the 60–145 m ( $\pm 12$  m) is more than one order of magnitude greater than the scaled initial diameters of streamers shown in Fig. 5c (at 60 km,  $2r_s \simeq 4$  m), given realistic charge moments available for the sprite initiation (Hu et al. 2002), it is likely that

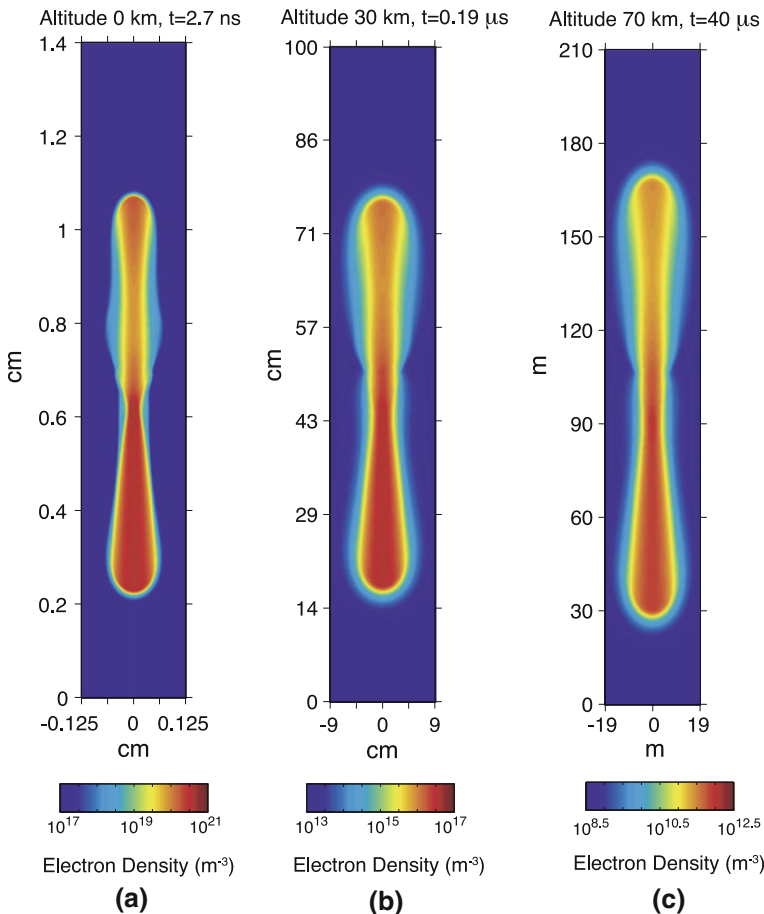


**Fig. 5** A cross-sectional view of the distribution of the electron number density of the model streamers at altitudes **a** 0 km, **b** 30 km, and **c** 70 km (Liu and Pasko 2004). Reprinted by permission from American Geophysical Union

streamers appearing at these low altitudes were initiated at much higher altitudes and propagated long distances experiencing substantial expansion (e.g., Liu et al. 2009a).

## 2.4 Avalanche-to-Streamer Transition

The classic Meek breakdown condition allows simple quantitative determination about when streamers can be formed from electron avalanches by evaluating the product of electric field-dependent Townsend ionization coefficient  $\alpha(E)$  [ $\text{m}^{-1}$ ] and discharge gap length  $d$  [m],  $\alpha(E) d \simeq 18\text{--}20$  (Meek 1940). Physically, this condition indicates when the electric field created by space charge of the avalanche becomes comparable to the externally applied field (e.g., Raizer 1991, p. 336). Montijn and Ebert (2006) recently emphasized the importance of inclusion of electron diffusion for quantitative description of the avalanche-to-streamer transition. Qin et al. (2011) have noted that in order to monitor the inception of sprite streamers, which cannot be modeled with present computer resources in the framework of fluid models, it is critical to accurately quantify avalanche-to-streamer transition processes. In particular, it is critical to accurately quantify the growth of the avalanches initiated by preexisting plasma inhomogeneities at lower ionospheric altitudes (see further discussion in Sect. 3.2). Given the broad range of length scales involved in the problem, and the related numerical requirements, an alternative way to performing the plasma fluid modeling is to employ a criterion on the particle level to check possible initiation of sprite streamers. In comparison with previous work, Qin et al. (2011) introduced a simple numerical procedure (summarized below) based on the solution of two ordinary differential equations, which allowed effective monitoring of streamer initiation for arbitrary either time or spatial variation of the applied electric field, and accounting for space charge repulsion and diffusion of the avalanche.

An avalanche of electrons is approximated by a sphere with time-dependent radius  $R_a$  that is described by the ordinary differential equation (Qin et al. 2011):

$$\frac{dR_a}{dt} = \mu_e E' + \frac{2D_e}{R_a} \tag{1}$$

where  $\mu_e$  and  $D_e$  are the mobility and the diffusion coefficient of electrons, respectively, and  $E' = \frac{q_e N_e}{4\pi\epsilon_0 R_a^2}$  is the space charge field of the avalanche, where  $N_e$  and  $q_e$ , respectively, represent the total number of electrons inside the avalanche and the absolute value of the charge of the electron. The related geometry is illustrated in Fig. 6. The first term on the right-hand side of (1) describes the expansion of the electron avalanche due to electrostatic repulsion. The second term accounts for the effects of diffusive spreading of the avalanche. We note that, in the absence of repulsion force, the solution of Eq. (1) correctly captures classic diffusive expansion of the radius  $R_a^2 = R_{a0}^2 + 4D_e t$ , where  $R_{a0}$  is the effective initial radius of electron cloud. The initial avalanche size  $R_{a0}$  does not affect the results as long as it is chosen so that the initial space charge field of the avalanche is much smaller than the breakdown field. The time dynamics of  $N_e$  is described by the following equation:

$$\frac{dN_e}{dt} = (v_i - v_a) N_e \tag{2}$$

where  $v_i$  and  $v_a$  are ionization and two-body dissociative attachment frequencies, respectively. Three-body attachment processes are negligible at air pressure corresponding to mesospheric/lower ionospheric altitudes. It was assumed in (Qin et al. 2011) that  $E' \geq E_k/3$  corresponds to the avalanche-to-streamer transition (Raizer 1991, Section 12.2.6). This is a



Mainly due to the increasing radius of the streamer head of an accelerating streamer, the brightness of the streamer head increases as well (see Fig. 7). The results reported in Liu et al. (2009a) demonstrate that the brightness of a sprite streamer head increases exponentially with time and can span more than 4 orders of magnitude in a very short period of about 1 ms. The rate of increase depends on the magnitude of the applied electric field. Liu et al. (2009a) proposed a method for remote sensing of the sprite-driving electric field in the mesospheric and lower ionospheric region by measuring the rate of the change of the brightness. In particular, Liu et al. (2009a) reported that the sprite event presented in McHarg et al. (2007) and Stenbaek-Nielsen et al. (2007) was initiated by fields close to the conventional breakdown threshold  $E_k$ . Qin et al. (2012c) recently suggested that, in addition to optical manifestation, the exponential growth of sprite streamers is associated with exponential growth of streamer current, which can radiate electromagnetic radiation in the low-frequency (LF, 30–300 kHz) band for strong positive cloud-to-ground lightning discharges, allowing propagation of sprite streamers to low altitudes  $\leq 40$  km.

Luque and Ebert (2010) applied a model with adaptively refined grids to study the propagation of long sprite streamers with transverse dimension on the order of 1 km through the altitude range with a significant variation of ambient air density. Luque and Ebert (2010) assumed a constant electric field as a function of altitude (40 V/m) and observed that, in their model, the optical emission intensity varied proportionally to air density and therefore exponentially in time for the streamer with velocity and radius that remained relatively stable. We note that due to the assumed large initial dimension of model streamers ( $\approx 1$  km), modeling results of Luque and Ebert (2010) do not capture the experimentally observed initial acceleration of streamers and more than two orders of magnitude increase in their brightness, which are believed to be the results of exponential expansion of streamers with time constant  $\sim 0.1$ – $0.2$  ms and over relatively short distances  $\leq 3$  km (i.e., not exceeding the atmospheric scale height) when streamers grow from initial seeds with several tens of meters dimensions (e.g., Liu et al. 2009a; Kosar et al. 2012). The modeled streamer transverse dimension of 1 km exceeds the experimentally measured transverse dimensions  $\sim 400$  m of streamers propagating without branching (McHarg et al. 2010) in the same altitude range as considered in Luque and Ebert (2010).

We note that the exponential expansion and acceleration of streamers is an important effect that was recently identified to be also accompanied by exponential growth of electric potential differences in the streamer heads (Celestin and Pasko 2011). These electric

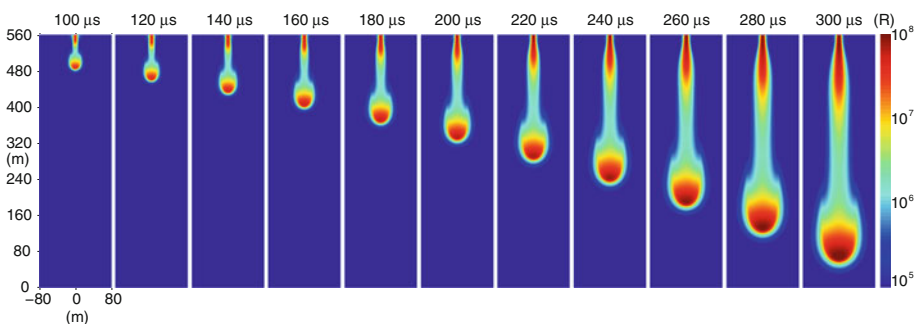


**Fig. 7** A time sequence of intensity distributions in Rayleighs of the first positive band system of  $N_2$  for a downward propagating model positive streamer at 75 km altitude (Liu et al. 2009a). The sequence of images is shown with 20- $\mu$ s interval, starting at 100  $\mu$ s and ending at 300  $\mu$ s. The formatting is consistent with that of Fig. 2 of Stenbaek-Nielsen et al. (2007). Reprinted by permission from American Geophysical Union

potential differences have significant implications for the energy that thermal runaway electrons can gain once created and quantitative results of Celestin and Pasko (2011) indicate that under realistic conditions associated with lightning leaders, streamers can create  $\sim 100$  keV electrons capable of further acceleration to several MeVs energies needed for the explanation of terrestrial gamma ray flashes (TGFs) in the Earth's atmosphere (e.g., Fishman et al. 1994; Smith et al. 2005). We note that the energy of photons in TGFs can reach up to 100 MeV (Tavani et al. 2011), and the most recent observations indicate that many TGFs are produced during upward negative leader progression prevalent in normal polarity intra-cloud flashes (Lu et al. 2010, 2011).

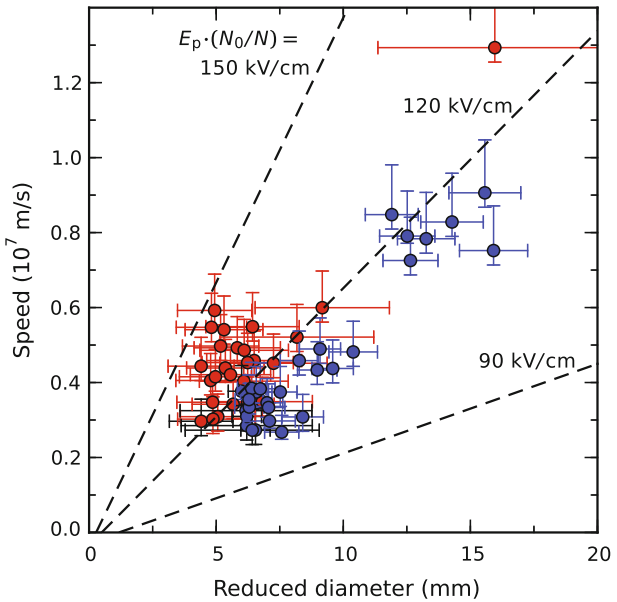
Kanmae et al. (2012) have recently explored the diameter–speed relationship of sprite streamers based on triangulated high-speed observations in July 2010. The sprite streamers were observed using two intensified high-speed cameras recording at 10,000 and 16,000 frames per second in addition to two low-light level video cameras deployed at two remote sites and used for triangulation of sprites. More information on the triangulation technique can be found in Stenbaek-Nielsen et al. (2010). According to Kanmae et al. (2012), the uncertainty range on the altitude of the triangulated objects is as low as 0.6 km, while the lowest pixel resolution is 17 m. Using this system, Kanmae et al. (2012) were able to perform accurate measurements of sprite streamer diameters ( $D$ ) and velocities ( $V_S$ ). They have found that bigger streamers tended to involve higher speeds in a linear fashion. Owing to their triangulation technique, they were able to go further and scale the streamer diameters with respect to the air density ( $D \times N/N_0$ ) and plot this quantity with respect to  $V_S$  (see Fig. 8). Naidis (2009) suggested that it is possible to evaluate the peak electric field in a streamer head if one knows the streamer diameter and velocity simultaneously, and proposed a relation that linked these three quantities (dashed lines in Fig. 8). Using this idea, Kanmae et al. (2012) used their measurements in order to evaluate the electric field in streamer heads (see additional discussion on this topic in Sect. 3.8). They found peak electric fields from 3 to 5 times the breakdown threshold  $E_k$ , which is in good agreement with simulations (e.g., Liu et al. 2006).

We note that the linear relationship between  $D$  and  $V_S$  was discussed in Liu and Pasko (2004) and was also used by Liu et al. (2009a) to show the consistency between sprite streamer models and observations, as well as to develop a new remote sensing technique to probe the sprite-driving ambient electric field in the mesosphere. As was noted above in this section, Liu et al. (2009a) showed that the diameter and the luminosity of sprite streamers varied exponentially with time, and that the exponential rate of this increase could be used to determine the reduced sprite-driving ambient electric field. It is interesting to point that applying both techniques described by Kanmae et al. (2012) and Liu et al. (2009a) to a given observed sprite would lead to the determination of the peak electric fields in the sprite streamer head and simultaneously the sprite-driving ambient electric field, therefore leading to a very good characterization of the sprite streamers.

Additionally, Kanmae et al. (2012) have observed that narrow sprite streamers rarely split and some of them even exhibit deceleration of approximately  $10^9$  m s<sup>-2</sup>. Comparatively, Li and Cummer (2009) recorded decelerations of sprite streamers in a different observation campaign of approximately  $10^{10}$  m s<sup>-2</sup>, but one ought to note that these values should depend on the exact ambient electric field in which these streamers propagate. Nevertheless, Li and Cummer (2009) and Kanmae et al. (2012) measured consistent minimum velocities for the dimmest/narrowest sprite streamers on the order of  $10^6$  m s<sup>-1</sup> and consistent maximum velocities on the order of  $10^7$  m s<sup>-1</sup>.

In contrast to the observation of narrow streamers, Kanmae et al. (2012) also noted that expanding sprite streamers would branch into multiple daughter streamers with a greater

**Fig. 8** The speed  $V_S$  as a function of reduced diameter  $D \times (N/N_0)$  for two observed sprite events on July 14, 2010 occurring over a large thunderstorm near the southeastern corner of Arizona at 04:29:32 UT (blue) and at 04:39:33 UT (red). The reduced diameters plotted with black error bars are at the upper limits of the measurement. Lines are obtained from the model of Naidis (2009) (see text) evaluated at selected peak electric fields in the streamer head (Kanmae et al. 2012). Reprinted with permission of IOP Publishing



number than those for laboratory streamers at ground pressure. In their study, they also observed that the diameters of sprite streamers (scaled with the air density) are larger than their ground pressure counterparts. As predicted by Liu and Pasko (2004, 2006), these results possibly indicate a deviation from the similarity laws due to the quenching of the excited states of nitrogen responsible for the photoionization process below  $\sim 25$  km altitude.

### 3.2 Initiation of Positive and Negative Streamers in Sprites

Although it has been suggested that sprites may be initiated through simultaneous up and down propagating streamers (Liu and Pasko 2004), the recent observational evidence indicates that the preferential form of sprite initiation is through downward development of positive streamers launched in the region of the lower ledge of the Earth's ionosphere [see discussion in (Stenbaek-Nielsen et al. 2007; McHarg et al. 2011)]. The exact mechanism of initiation of sprite streamers is still not well understood and related recent studies are reviewed below. The mechanism may be related to the formation of upwardly concave ionization regions near the lower ionospheric boundary associated with sprite halos (Barrington-Leigh et al. 2001). As was discussed recently in Pasko (2010), the double-headed streamers may be involved in initiation of sprites; however, due to the fast exponential increase in streamer brightness in time (see review of Liu et al. (2009a) above), the initial appearance of positive streamers is likely realized because of a relatively slow application of the electric field at sprite altitudes (duration  $\sim 1$  ms) (Marshall and Inan 2006; Hu et al. 2007) coupled with lower propagation threshold for positive streamers in comparison with negative ones (Pasko et al. 2000). This creates asymmetric conditions with predominant initial propagation of positive streamers. Other factors have also been proposed, and a review of recent research work on this subject is provided below.

Luque and Ebert (2009) have recently reported a high-resolution modeling of inception of sprite streamers as a result of sharpening and collapse of screening-ionization wave

associated with a sprite halo. The streamer emerged as a result of halo dynamics on the axis of symmetry in a two-dimensional axisymmetric plasma fluid model that employed a nonuniform, dynamically adapted computational grid (Luque and Ebert 2009). The transverse dimension of the modeled streamer was on the order of 1 km, and its time dynamics was resolved on a fine grid with  $\geq 3$  m spatial resolution (Luque and Ebert 2009). This result is qualitatively similar to the dynamics reported in early low-resolution sprite modeling in which columns of ionization with transverse extent on the order of 10 km, were observed to emerge from upwardly concave regions of sprites and to propagate down to altitudes  $\sim 45$  km (Pasko et al. 1996). We note that, although the upwardly concave regions of luminosity forming during sprite development were fully resolved and quantitatively described in early papers (Pasko et al. 1995, 1996, 1997; Veronis et al. 2001), the name sprite halo that is now used in association with these events was introduced several years later when these events, driven primarily by quasi-static electric fields, were experimentally discovered, clearly identified, and separated from elves phenomena using comparisons of high-speed video observations and fully electromagnetic modeling (see discussion in Barrington-Leigh et al. 2001, and references cited therein). A significant difficulty of both the early (Pasko et al. 1996) and more recent (Luque and Ebert 2009) modeling is that streamers appear in these models as a continuous process of halo development, while in many existing high-resolution photometric and video records, the sprite streamers exhibit significant spatial (both vertical and horizontal) as well as temporal separations with respect to position and timing of the sprite halo (Qin et al. 2011, and extensive list of references therein). The asymmetry in initiation of sprite streamers by cloud-to-ground lightning discharges with different polarities and sprite streamers triggered by cloud-to-ground lightning with very low charge moment changes are also not reproduced by models reported by Pasko et al. (1996) and Luque and Ebert (2009). Additionally, Qin et al. (2011) recently indicated that the collapse of sprite halo reported in (Pasko et al. 1996; Luque and Ebert 2009) is due to numerical instability, which can be somewhat postponed but not eliminated by increasing resolution of numerical grid.

In order to monitor the inception of sprite streamers, which cannot be modeled with present computer resources in the framework of fluid models, Qin et al. (2011) have used an improved avalanche-to-streamer transition criterion and have investigated the response of the lower ionosphere to the charge moment changes induced by lightning discharges as a system of avalanches. Qin et al. (2011) established a direct link between the charge moment change and the ambient electron density profile as required for triggering of sprite streamers. The related condition is defined as  $h_{\text{tran}} \geq h_{\text{cr}}$ , where  $h_{\text{tran}}$  represents the altitude at which the electron density is low enough so that the distance between electrons is equal to the radius of the electron avalanche at the moment of avalanche-to-streamer transition, and  $h_{\text{cr}}$  represents the altitude at which the ambient electric field  $E_0$  created by the charge moment change in the thunderstorm is equal to the conventional breakdown field  $E_k$ . An analysis of the origin of polarity asymmetry between +CGs and -CGs in triggering for sprite streamers conducted by Qin et al. (2011) indicated that the vertical extent of the streamer initiation region (SIR) created by a -CG was smaller than the SIR created by the opposite +CG that corresponded to the same charge moment change. This is due to the fact that the positive SIR is basically equivalent to the high field  $E_0 > E_k$  region created by the halo because upward avalanches generated in a low-electron-density region can penetrate deep into the high-electron-density region of the halo. In contrast, the negative SIR is limited to the high field region where the electron density is low enough for avalanches to develop without overlapping. Qin et al. (2011) also demonstrated as part of the asymmetry study that the triggering of long-delayed sprites is a unique property of halos produced by

positive cloud-to-ground lightning discharges due to the formation of a long-lasting high field region that can be significantly enlarged by the lightning continuing current. Qin et al. (2011) demonstrated the importance of initial inhomogeneities in the lower ionosphere for the initiation of sprite streamers and indicated that a large number of initial seed electrons distributed in a compact region of space  $N_{0e}$  creates more favorable conditions for the initiation of sprite streamers. It is important to emphasize that the initial inhomogeneities were discussed in many early papers on sprite modeling (Pasko et al. 1996, 1997; Raizer et al. 1998; Zabolin and Wright 2001; Raizer et al. 2010). Raizer et al. (1998, 2010), for example, introduced a seed inhomogeneity with radius 60 m and electron density  $150 \text{ cm}^{-3}$  (corresponding to  $N_{0e} \sim 10^{14}$ ) at 80 km altitude. The approach of Qin et al. (2011) is different as it considers the seed electrons in the framework of competition of many avalanches in which only a perturbation with a larger number of initial electrons reaches the avalanche-to-streamer transition, becomes dominant in defining the macroscopic electric field, and also eventually becomes observable. Qin et al. (2011) quantitatively demonstrated that in the framework of avalanche-to-streamer transition, even values twelve orders of magnitude lower than those employed by Raizer et al. (1998, 2010) (i.e.,  $N_{0e} \sim 10^2$ ) play a definitive role in initiation of sprite streamers. The possible role of inhomogeneities in electron density in the formation of bright beads and branching of sprite streamers has recently been discussed by Luque and Gordillo-Vazquez (2011).

As was already mentioned in this and the preceding subsection, the sprite streamers initiate from electron inhomogeneities in the lower ionosphere and undergo significant acceleration and expansion growth before their optical emissions become observable. Qin et al. (2012a) demonstrated recently that electron inhomogeneities located at high altitudes in the region of sprite halo, which may be subvisual, only transform into single-headed downward streamers, and corresponding upward streamers quickly merge into the sprite halo due to fast relaxation of lightning-induced electric field. In contrast, the inhomogeneities located at and below the lower edge of the sprite halo, where a high field region persists significantly longer, can transform into double-headed streamers (Qin et al. 2012a). The upward negative streamer heads start from the existing bright structures in the channel of previous downward streamers as observed by Cummer et al. (2006), McHarg et al. (2007) and Stenbaek-Nielsen and McHarg (2008) because, at low altitudes, electron density enhancements associated with these channels are much stronger than in preexisting inhomogeneities in the ambient ionosphere. Figure 9 provides a schematic summary of the above-discussed scenarios. Figure 10 provides a model illustration of differences in initiation of single-headed (initial altitude of inhomogeneity 77.25 km, left panel) and double-headed (initial altitude of inhomogeneity 75.25 km, right panel) streamers for a charge moment change of 600 C km. We note that the scale shown by a color bar underneath the panels in Fig. 10 is a logarithmic scale. The streamers that are observed in sprites usually go through a relatively short stage of exponential growth before their optical emissions become observable (Liu et al. 2009a) (see Fig. 7). The growth is significant (i.e., four orders of magnitude as was demonstrated in Liu et al. (2009a)). In both the left and right panels of Fig. 10, one can see initial stage of this growth vividly for the downward going positive streamers. As streamer gets in this regime, it continues to grow exponentially. The process has very sharp dependence on ambient conditions—if the duration of the electric field is short and ambient electron density is high as at high altitude in the sprite halo, streamer weakens, does not expand/grow, and is not visible/observable. This is why the upward streamers are different in left and right panels of Fig. 10. The left panel shows upward streamer that does not grow and fades, but the right panel shows an upward streamer that is fully formed and continues its exponential growth (Qin et al. 2012a).

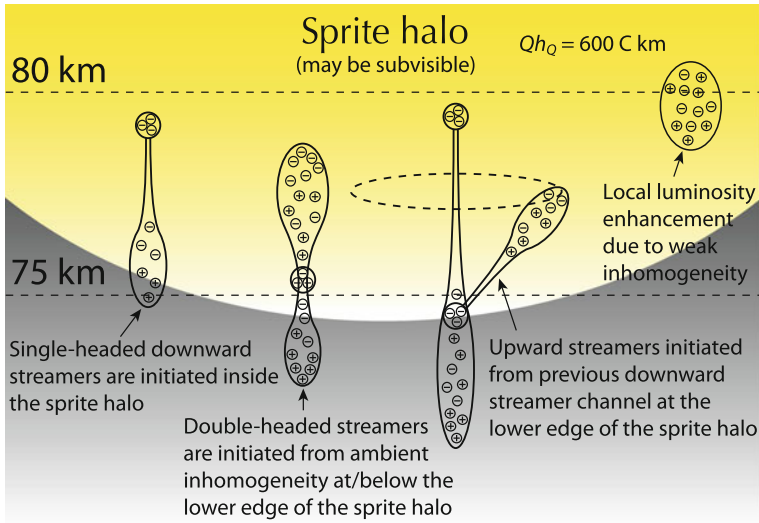


**Fig. 9** Schematic illustration of development of either single- or double-headed streamers depending on altitude position of initial inhomogeneity with respect to sprite halo (Qin et al. 2012a)

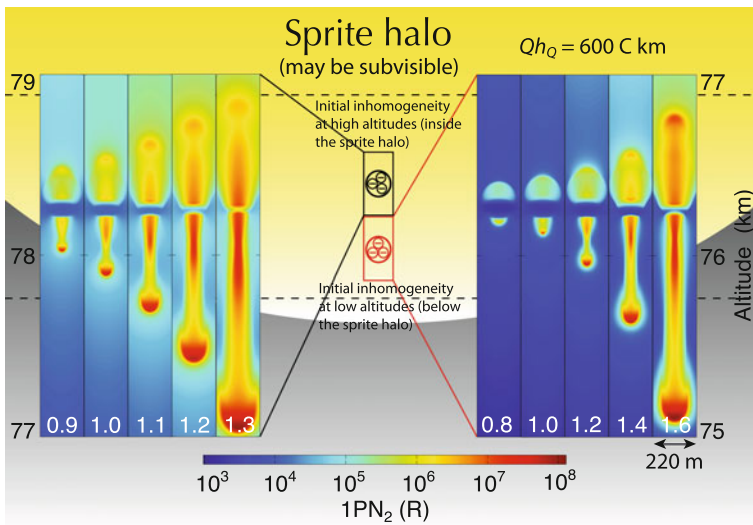


**Fig. 10** Cross-sectional views of optical emissions of the first positive band system of  $N_2$  in Rayleighs produced by streamers initiated from inhomogeneities that are located at 77.25 km (left panel) and 75.25 km (right panel), respectively (Qin et al. 2012a)

Note that when demonstrating the necessity of preexisting plasma inhomogeneities in the initiation of sprite streamers in Qin et al. (2011, 2012a), the plasma density in the inhomogeneities is assumed to have a spherical Gaussian distribution. Liu et al. (2012) emphasized that the shape of the inhomogeneities has a significant impact on the initiation of sprite streamers, especially in sub-breakdown conditions. These authors studied the

initiation of streamers from vertically elongated ionization columns at sub-breakdown conditions (i.e., in a uniform applied electric field,  $E < E_k$ , where  $E_k$  is the conventional breakdown field) and found that the polarization of the ionization columns produces significant space charge field that enables streamer initiation at the tip of the columns. Figure 11 shows an example of streamer initiation at 70 km altitude in applied field  $E_0 \simeq 0.5E_k$  (Liu et al. 2012). Liu et al. (2012) estimated the requirements for the dimension and density of the initial column for streamer initiation and showed that the length  $l$  of the column could be approximated by

$$l = a \left[ \frac{1}{0.56} (E_m/E_0 - 3) \right]^{1/0.92} \tag{3}$$

where  $E_m$  corresponds to typical field around the streamer head  $\sim 3\text{--}5E_k$ , and the peak plasma densities  $n_{e0}$  and  $n_{p0}$  in the ionization column should be

$$n_{e0} = n_{p0} = \frac{2\epsilon_0(3a + l)E_0}{q_e\pi^{0.5}a^2} \tag{4}$$

where  $q_e$  is the charge of the electron,  $a$  is the radius of the ionization column, and  $E_0$  is the magnitude of the uniform ambient electric field (Liu et al. 2012). Liu et al. (2012) suggested that the proposed mechanism related to the initiation of streamers at sub-breakdown conditions may explain the initiation of lightning flashes in the troposphere where the measured ambient electric field is well known to be below conventional breakdown field, as well as the initiation of sprite streamers in the lower ionosphere in the case of a lightning-induced electric field of  $0.2\text{--}0.6E_k$ .

### 3.3 Afterglow Region in Sprite Streamers

Liu (2010) has recently discussed the mechanisms for the luminous trail or “afterglow” region often observed at higher altitudes in downward propagating sprite streamers (McHarg et al. 2007; Stenbaek-Nielsen et al. 2007). The physical mechanisms of the

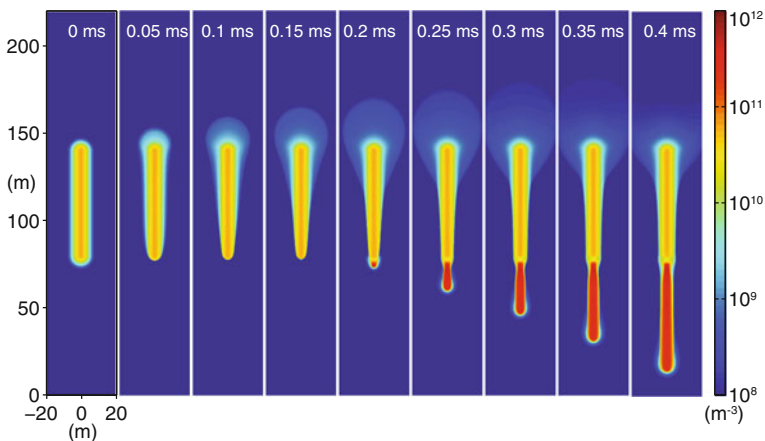


**Fig. 11** Cross-sectional views of distributions of electron density during the initiation of a sprite streamer at 70 km altitude in applied 5 km field  $E_0 \simeq 0.5E_k$  (Liu et al. 2012). Copyright 2012 by the American Physical Society

observed phenomenon discussed in the existing literature include emissions produced due to energy transfer from  $N_2$  and  $O_2$  metastable electronic states, energy pooling between low energy metastable states, and energy pooling between the metastable states and the vibrationally excited ground electronic state of  $N_2$  (e.g., Morrill et al. 1998; Bucselá et al. 2003; Kanmae et al. 2007; Pasko 2007; Sentman et al. 2008; Sentman and Stenbaek-Nielsen 2009). Liu (2010) demonstrates that the luminous trail also naturally appears in numerical modeling of sprite streamers in which the above-mentioned chemical processes are not taken into account. The effect is due to increase in current that flows in the sprite streamer body when streamer expands, accelerates, and brightens. The increasing current self-consistently leads to the rise of the electric field in the streamer channel far behind the streamer head, which leads to effective production of  $N_2$  excited states by electron impact excitation and then to the glowing trail (Liu 2010).

The results of Liu (2010) concerning the luminous trail are in agreement with more recent work of Luque and Ebert (2010) reviewed in Sect. 3.1. Luque and Ebert (2010) also observed a negative charging of the upper section of the positive streamer that propagated downward and suggested that this negative charging may facilitate the emergence of upward negative streamers and attraction of positive streamer heads to previously formed channels as observed experimentally (Luque and Ebert 2010, and references therein).

Li and Cummer (2011) have recently used lightning-driven background electric fields at mesospheric altitudes deduced from ELF electromagnetic measurements in combination with high-speed images of sprite streamers to estimate charges that are present in bright columnar cores appearing at the upper extremities of sprites. The analysis assumed that the observed negative streamers that emerge from the bright negatively charged cores propagate along the directions of the local electric field lines, and the amount and vertical distributions of charge were iterated until good agreement was achieved with high-speed video images in terms of angles of emergence of negative streamers with respect to the vertical cores. The authors were able to establish a lower bound on the electric charge in six observed sprites driven by positive lightning. They found, in particular, that individual bright sprite cores contain significant negative space charge between  $-0.01$  and  $-0.03$  C. Given the significant negative charge, Li and Cummer (2011) interpreted the sprite core region as the partial and perhaps dominant sink of the negative charge created by the downward positive polarity streamers. This further suggests that when downward streamers supply more charge than can be absorbed by the sprite core, slightly delayed upward negative streamers initiate from the sprite core to disperse this charge (Li and Cummer 2011). This is consistent with observations that show that the subsequent upward streamers are not always present, especially in smaller sprites (Li and Cummer 2011). The findings of Li and Cummer (2011) that the emergence of secondary negative streamers may be related to the negative charging of the upper section of the downward positive streamers are consistent with similar ideas advanced in (Luque and Ebert 2010). An important original finding of the analysis of Li and Cummer (2011) is that it allowed for the first time to use sprite imagery to find whether approximately 10-km-long bright sprite core regions were electrically attached to the high-conductivity regions of the lower ionosphere. The analysis indicated a weak or nonexistent electrical connection between the ionosphere and the downward streamers (Li and Cummer 2011). In addition to other important factors discussed above in the context of halo-streamer transition (Pasko et al. 1996; Luque and Ebert 2009), the new findings of Li and Cummer (2011) also support the idea that sprite streamers do not represent a continuous process of sprite halo development as they appear to be disconnected from the high conductivity region of the Earth's ionosphere above.

Following the work of Liu et al. (2012), Kosar et al. (2012) further investigated sprite streamer formation at sub-breakdown conditions and emphasized specifically the brightening of the initial isolated ionization columns following streamer formation as an explanation for the persistent luminous trails left by positive streamer heads in sprites (i.e., afterglow region in sprite streamers). The brightening of the ionization columns results from the exponential increases of the total current flowing along the streamer body as the streamer accelerates, expands, and brightens, leading to the increase of the electric field in the column (Liu and Pasko 2010; Kosar et al. 2012). Kosar et al. (2012) have also investigated the exponential growth rates of the sprite streamers initiated at sub-breakdown conditions and concluded that the exponential growth rates of speed and brightness of the streamer heads are mainly determined by the magnitude of the ambient electric field and scale with neutral air density as  $\sim N$ . We note that both Liu et al. (2012) and Kosar et al. (2012) emphasized that it is more difficult to initiate negative streamers than positive streamers, as negative streamers do not initiate on the timescale of their simulations even if the ambient field is as large as  $0.8E_k$ . These authors conjectured that the initiation of negative streamers might occur at a later moment of time due to the accumulation of negative charge around the origin of the positive streamer with a rate faster than its dissipation during the propagation of positive streamers. This inception mechanism of negative streamers in sprites is different from the one proposed by Qin et al. (2013) who considered initiation of negative streamers from preexisting ionization patches or from high-electron-density channels produced by previous positive streamers under the conditions of a sufficiently large ambient field of  $\gtrsim 0.8E_k$  that persists longer than  $\sim 2$  ms.

### 3.4 Carrot and Columniform Sprites

Carrot sprites, exhibiting both upward and downward propagating streamers, and columniform sprites, characterized by predominantly vertical downward streamers, represent two distinct morphological classes of lightning-driven transient luminous events in the upper atmosphere. Figure 12 illustrates double-headed and single-headed streamer initiation regions (SIRs) corresponding to the production of carrot and columniform sprites, respectively, assuming different values of charge moment changes  $Qh_Q$  and an impulsive lightning discharge with duration of 1 ms (Qin et al. 2013). This particular study assumed the ambient electron density profile (Wait and Spies 1964):

$$n_e(h) = 1.43 \times 10^{13} e^{-0.15h'} e^{(\beta-0.15)(h-h')} [m^{-3}] \quad (5)$$

where  $h' = 85$  km and  $\beta = 0.5 \text{ km}^{-1}$  are parameters describing reference altitude and sharpness for a typical nighttime electron density profile (e.g., Han and Cummer 2010), and  $h$  is the altitude variable.

In order to divide the upper atmosphere into different streamer initiation regions, Qin et al. (2013) placed test inhomogeneities at different mesospheric altitudes and simulated their evolution under the application of lightning-induced electric field  $\mathbf{E}_{\text{halo}}(r, z, t)$  (see discussion at the end of Sect. 2.4 about the two-step simulation technique). Figure 12 shows the subdivisions for a given Gaussian plasma inhomogeneity with peak density  $2 \times 10^9 \text{ m}^{-3}$  and a characteristic radius 30 m (Qin et al. 2013). For positive cloud-to-ground lightning discharges (+CGs) that produce large charge moment changes, such as the cases shown in Fig. 12a, b, c, the upper atmosphere can be divided into four sub-SIRs. An important feature in these cases is that Double-SIRs are present and each is sandwiched

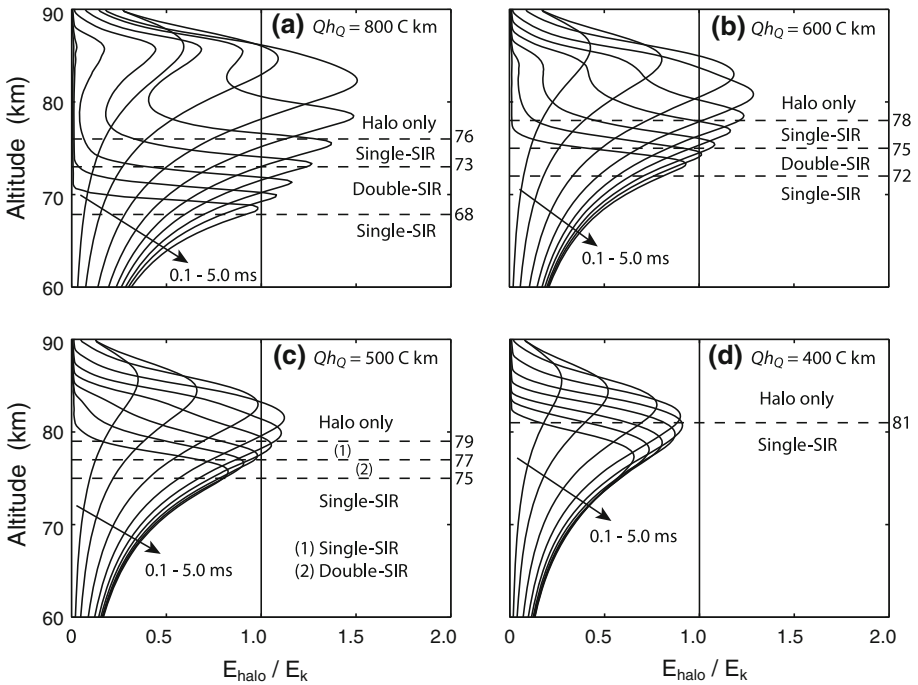


**Fig. 12** Reduced electric field  $E_{\text{halo}}/E_k$  along the axis of symmetry of sprite halos at  $t = 0.1, 0.2, 0.4, 0.7, 1.1, 1.6, 2.4, 3.4, 5.0$  ms produced by +CGs associated with total charge moment changes of **a** 800 C km, **b** 600 C km, **c** 500 C km, and **d** 400 C km, and division of the upper atmosphere into different sub-SIRs for a given Gaussian plasma inhomogeneity with peak density  $2 \times 10^9 \text{ m}^{-3}$  and characteristic radius of 30 m. “Single-SIR” and “Double-SIR” denote single- and double-headed streamer initiation region, respectively (Qin et al. 2013). Reprinted by permission from American Geophysical Union

by two Single-SIRs. We note that the presence of Double-SIR is a necessary condition for the initiation of upward negative streamers and therefore the formation of carrot sprites.

Qin et al. (2013) found that upward negative streamers are only able to initiate in a region where the mesospheric electric field  $E_{\text{halo}}(r, z, t)$  persists with  $\geq 0.8E_k$  for  $\geq 2$  ms, whereas downward positive streamers are able to initiate as long as  $E_{\text{halo}}(r, z, t)$  persists with  $\geq 0.5E_k$  for several milliseconds. This difference leads to two important results shown in Fig. 12d. First, in the case of a +CG with a small charge moment change such as 400 C km, the double-SIR is absent due to the fact that the entire lower ionosphere is under sub-breakdown condition (see Fig. 12d), and it is found that  $\sim 500$  C km is the minimum charge moment change that can produce carrot sprites under typical nighttime conditions (i.e.,  $h' = 85 \text{ km}$  and  $\beta = 0.5 \text{ km}^{-1}$ ). Second, for large charge moment changes such as 800 C km, it is expected that carrot sprites are able to initiate close to the center of the sprite halo in a region where the lightning-induced electric field persists at above  $\sim 0.8E_k$  for  $\geq 2$  ms, whereas in the same event, columniform sprites may appear at the periphery of the sprite halo where the electric field lasts for only  $\sim 1$  ms above  $0.8E_k$  or persists at  $0.5E_k$   $\geq E_{\text{halo}} \geq 0.8E_k$  for several milliseconds (see additional results and discussion in (Qin et al. 2013; Vadislavsky et al. 2009)). We also note that in the context of this discussion, the inhomogeneity is placed in the upper Single-SIR in the left panel and in the Double-SIR in the right panel of Fig. 10 discussed in Sect. 3.2.

Qin et al. (2013) also established that, for a sufficiently large  $Qh_Q$ , the time dynamics of the  $Qh_Q$  determines the specific shape of the carrot sprites. In the case when the sufficiently large  $Qh_Q$  is produced mainly by an impulsive return stroke, a strong electric field is produced at high altitudes and manifests as a bright halo, and the corresponding conductivity enhancement lowers/enhances the probability of streamer initiation inside/below the sprite halo. A more impulsive return stroke leads to a more significant conductivity enhancement (i.e., a brighter halo). This conductivity enhancement also leads to fast decay and termination of the upper diffuse region of carrot sprites because it effectively screens out the electric field at high altitudes. On the contrary, if the sufficiently large  $Qh_Q$  is produced by a weak return stroke (i.e., a dim halo) accompanied by intense continuing current, the lightning-induced electric field at high altitudes persists at a level that is comparable to  $E_k$ , and therefore an extensive upper diffuse region can develop (Qin et al. 2013).

### 3.5 Asymmetry in Initiation and Propagation of Sprite Streamers Produced by Cloud-to-Ground Lightning Discharges with Different Polarities

Williams et al. (2012) have recently discussed a sprite polarity paradox that emphasizes dramatic differences in observational statistics of sprites with well-developed streamer structures that are produced by positive and negative cloud-to-ground lightning discharges (CGs). The essence of the paradox is that a global survey of charge moment changes associated with  $-CGs$  indicates that there is a small, but non-negligible number of  $-CGs$  that have magnitudes of charge moment changes as large as those that are known to produce sprite discharges in case of  $+CGs$ . Williams et al. (2012) estimated that the number of  $-CGs$  possessing these properties is approximately 10 % of the related  $+CG$  population worldwide. The paradox is that sprites produced by  $-CGs$  are extremely rare (much less than 10 % mentioned above), with very few events observed over many years of ground and satellite-based observations worldwide (Williams et al. 2012, and references therein). Williams et al. (2012) also pointed to a significant number of observed halos produced by  $-CGs$  and emphasized the importance of more impulsive lightning currents in  $-CGs$  in facilitating this phenomenology. With respect to sprite halos, the results of Qin et al. (2013) reviewed in the previous subsection are generally consistent with ideas of Williams et al. (2012). Additionally, Qin et al. (2011, 2012a, 2013) provide evidence related to physics of streamers, not discussed by Williams et al. (2012), indicating that the significant differences in the development of sprite streamers in case of  $+CGs$  and  $-CGs$  are the most important factor for understanding why sprites produced by  $-CGs$  are so rare. The key factors for the understanding of polarity asymmetry of sprites are as follows: (1) The threshold charge moment changes of positive and negative sprites are, respectively,  $\sim 320$  and  $\sim 500$  C km under typical nighttime conditions (Qin et al. 2013); (2) A factor of 3 lower minimum electric field required for the propagation of positive streamers in comparison with negative streamers (the related information is summarized in Sect. 2.3 of this review; this plays a role in the observability of sprites (see (4)) in addition to the effects included in (1)); (3) Positive cloud-to-ground discharges much more frequently produce large charge moment changes (e.g., Cummer and Lyons 2005; Williams et al. 2007, 2012; Lu et al. 2012); (4) Observability of sprites is a significant factor as streamers in sprites go through a significant growth before they become observable (Liu et al. 2009a; Qin et al. 2012a).

It should also be emphasized that, for the initiation of both positive and negative sprites, a strong inhomogeneity should be present in the ambient ionosphere (Qin et al. 2012b, 2013) that by itself may represent a significant limiting factor for the initiation of sprites.

This also directly reiterates the idea that the charge moment change alone is a necessary but not sufficient factor for sprites (Lang et al. 2011) and the state of the lower ionosphere and presence of inhomogeneities are important factors, especially for low charge moment changes.

The charge moment changes above 500 C km estimated by Qin et al. (2013) for the initiation of negative sprites under typical nighttime conditions are rare according to the analysis of Williams et al. (2007) and Williams et al. (2012, Fig. 8), and do not even occur in the measurements reported by Lu et al. (2012). We note that Li et al. (2012) have recently reported that very impulsive  $-CGs$  (produced at least 450 C km charge moment change in 0.5 ms or less) associated with essentially no continuing current could indeed produce negative sprites. The charge moment changes responsible for the 6 negative sprites were 750, 1050, 600, 650, 460, 450 C km, in remarkable agreement with the prediction of  $\sim 500$  C km threshold by Qin et al. (2013).

The downward streamers in negative sprites appear to be dimmer than their upward counterparts due to a higher critical field required for the propagation of negative streamers (Qin et al. 2011; Li et al. 2012). As already discussed in Sect. 2.2 of this review, streamers in sprites may remain subvisual and many negative sprites may have been produced but left undetected by observational techniques employed. A simple estimate based on the charge moment change data documented by Williams et al. (2007) and the charge moment thresholds for positive and negative sprites derived by Qin et al. (2013) (respectively, 320 C km and 500 C km under typical nighttime conditions) leads to the theoretical result that  $\sim 5\%$  of sprites should be negative. However, it should be noted that due to the differences in fields required for the propagation/growth of streamers of different polarity (i.e., key factor (2) mentioned above) and the resultant intrinsic dimness of negative streamers propagating in a given field as compared to positive streamers (i.e., key factor (4) mentioned above, please see also Fig. 14b and related discussion in Sect. 3.6 that follows), this estimate must be considered as an upper limit for observations. More measurements and observations on the impulsiveness of sprite-producing  $-CGs$ , dim streamers in negative halos produced by  $-CGs$ , and the charge moment contrast of  $+CGs$  and  $-CGs$  are necessary to further test the theories of sprite asymmetry.

Most recent experimental evidence indicates that the impulsiveness of charge transfer by lightning (i.e., during the first 2 ms) as well as the follow-up charge transferred by a lightning continuing current on timescales of 10s of ms, both significantly affect large-scale dynamics of electric field at high altitudes and sprite initiation processes (Lang et al. 2011). The lightning-driven electric fields not only initiate sprite streamers at high altitudes but also control their propagation to lower altitudes until termination. The charge moment change dynamics derived from electromagnetic remote sensing of lightning can be used to infer the background lightning-driven electric fields during the full extent of downward propagation of sprite streamers. With respect to polarity asymmetry of sprites, two recent studies on this subject by Li and Cummer (2012) and Li et al. (2012) are of special interest as they directly highlight differences between downward positive streamers propagating in positive sprites and analogous downward negative streamers in negative sprites.

Figure 13 illustrates the analysis of Li and Cummer (2012) indicating that positive streamers for two sprite events produced by positive CGs advanced downward to altitudes approximately corresponding to  $0.05E_k$ . The field at the termination altitude of streamer is a factor of 3 lower than minimum field required for the propagation of positive streamers at the same altitude  $E_{cr}^+$  calculated assuming that the ground value 4.4 kV/cm is scaled with altitude directly proportionally to air density  $N$  (see discussion about  $E_{cr}^\pm$  in Sect. 2.3).

Similar analysis for downward negative streamers in negative sprites conducted in Li et al. (2012) indicates that negative streamers terminate at field values  $0.2\text{--}0.3E_k$  that are a factor 1.3–2 lower than minimum field required for the propagation of negative streamers  $E_{\text{cr}}^-$  calculated assuming scaled with air density ground value of 12.5 kV/cm. We note that, for above-discussed estimates, Li and Cummer (2012) and Li et al. (2012) assumed a ground value of  $E_k \simeq 3.14 \times 10^6 \text{V/m}$  based on a model of Moss et al. (2006). It is generally expected that collective action of space charge of many streamers at lower extremities of sprites is able to enhance the electric field at the bottom of a conducting sprite body for both positive and negative sprites, facilitating propagation of streamers downward several kilometers beyond the point where the originally applied electric field is equal to  $E_{\text{cr}}^+$  for positive sprites and  $E_{\text{cr}}^-$  for negative sprites, respectively, as was demonstrated in e.g., Pasko et al. (2000). It is interesting to note in this context that if values of  $E_{\text{cr}}^\pm$  discussed above and their scaling with  $N$  are correct, the positive sprites appear to be more conducting providing a stronger focusing/enhancement of electric field in comparison with negative ones.

### 3.6 Minimum Charge Moment Changes Producing Sprites

Measurements indicate that surprisingly small charge moment changes of  $\sim 200 \text{ C km}$  (e.g., Hu et al. 2002; Hayakawa et al. 2004), in positive cloud-to-ground lightning discharges (+CGs), can initiate sprites. Qin et al. (2012b) recently used a plasma fluid model developed in Qin et al. (2012a, 2013) and reviewed in previous subsections to demonstrate that, for a spherically symmetric initial electron density inhomogeneities, the initiation of sprites by such small charge moment changes is only possible when the ionospheric D-region electron density profile is characterized by a reference altitude  $h'$  greater than 90 km (see Sect. 3.4 for model definition of ionospheric electron density profile). Vertically elongated inhomogeneities are found to be more favorable for sprite initiation, consistent with recently published studies (Kosar et al. 2012; Liu et al. 2012). It is calculated that for the same ionospheric conditions (i.e., inhomogeneities and  $h'$  values) that lead to initiation of sprites by +CGs associated with  $\sim 200 \text{ C km}$  charge moment changes, the minimum charge moment change required for the initiation of sprites by –CGs is 300 C km (Qin et al. 2012b).

Figure 14a shows the simulated optical emissions of the first positive band system of  $\text{N}_2$  ( $1\text{PN}_2$ ) as well as the reduced electric field  $E/E_k$  on the axis of symmetry for a streamer initiated from an inhomogeneity under the conditions defined by  $Qh_Q = 200 \text{ C km}$  and  $h' = 91 \text{ km}$  (Qin et al. 2012b). The streamer shown in Fig. 14a is initiated at 84.25 km altitude. We note that the sprite onset altitude of  $\sim 84 \text{ km}$  is consistent with triangulation measurements of Stenbaek-Nielsen et al. (2010) and Kanmae et al. (2012) showing that sprites could have onset altitudes as high as 88 km.

Figure 14b shows the dynamics of a streamer initiated by a –CG associated with  $Qh_Q = 300 \text{ C km}$  under the same ambient conditions as in Fig. 14a (Qin et al. 2012b). It appears that the downward negative streamer shown in Fig. 14b is much more diffuse than the upward positive streamer shown in Fig. 14a, as well as the downward positive streamer shown in Fig. 14a. This is because the negative space charge, which defines the location and shape of the negative streamer head, is formed by radially spreading electrons, whereas the positive space charge in the positive streamer head is formed by almost motionless ions. This, combined with different directions of electron drift with respect to applied electric field, leads to more compact size and higher electric field in positive streamer head

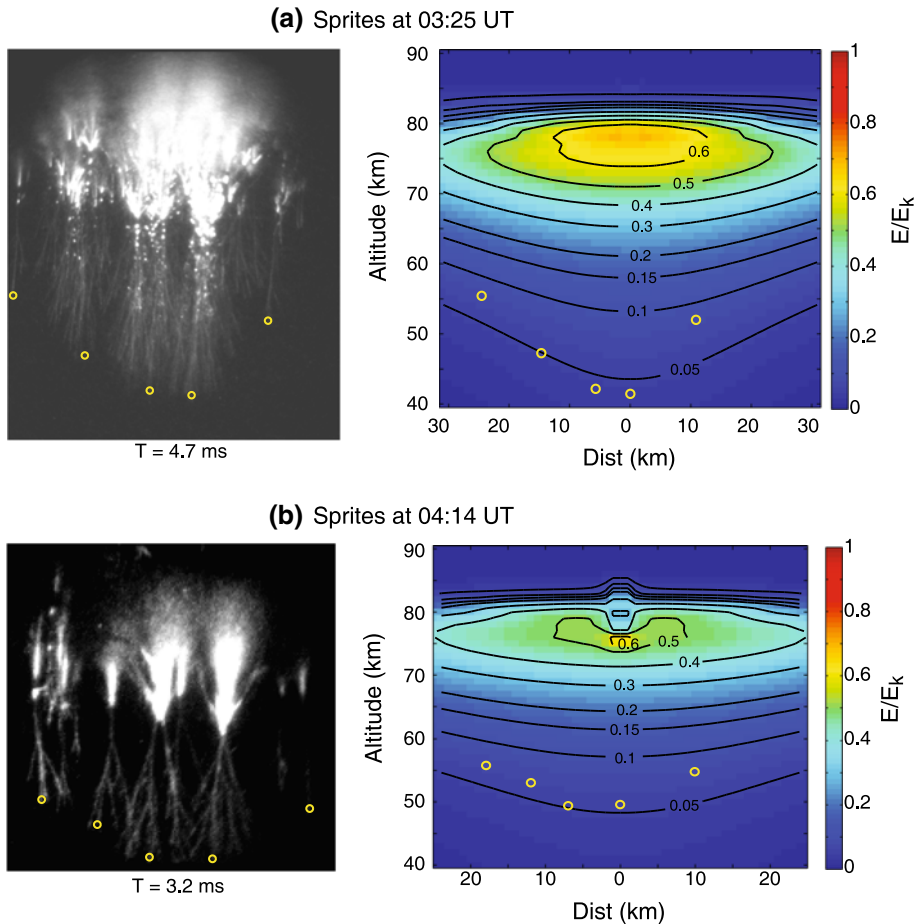


**Fig. 13** **a** High-speed image and inferred lightning-driven ambient electric fields for a sprite that occurred at 03:25 UT on August 13, 2005. *Left* high-speed images of different sprite elements fully developed at 4.7 ms after the parent lightning. *Right* normalized electric fields at the same instance. **b** High-speed image and inferred lightning-driven ambient electric fields for a sprite that occurred at 04:14 UT. *Left* high-speed images of different sprite elements fully developed at 3.2 ms after the parent lightning. *Right* normalized electric fields at the same instance. The *yellow circles* represent the termination location of each sprite element. The figure is adapted from (Li and Cummer 2012). Reprinted by permission from American Geophysical Union

in comparison with the negative one (e.g., Liu and Pasko 2004) as evident in Fig. 14. During the inception stage, the space charge in the negative streamer head is distributed in a larger volume and thus creates smaller electric field, when compared to that in the positive streamer head. Moreover, the weaker space charge field in negative streamers is also responsible for the fact that the initiation of negative sprites requires larger charge moment changes (i.e., higher external field) than that for positive sprites, since the total electric field in the streamer head must be higher than the conventional breakdown field  $E_k$  to create a region dominated by ionization.

To conclude discussion in this subsection, we note that results presented in Fig. 14b are similar to those in Fig. 7b in Qin et al. (2013) and provide a good visual illustration of

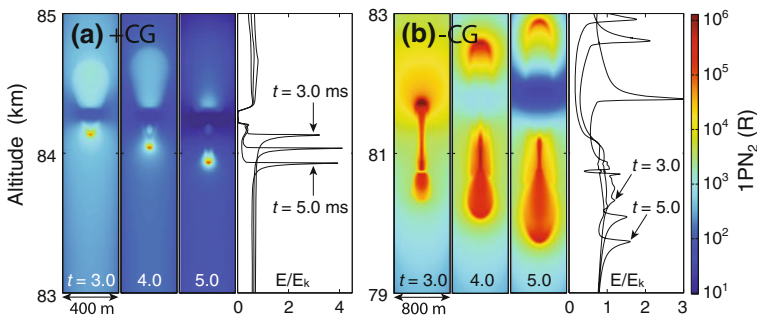


**Fig. 14** Cross-sectional view of optical emissions and reduced electric field  $E/E_k$  on the axis of symmetry for a streamer produced by **a** a +CG associated with  $Qh_O$  of 200 C km, and **b** a -CG associated with  $Qh_O$  of 300 C km. All the other conditions in these two cases are the same. The electron density profile is characterized by  $h' = 91 \text{ km}^{-1}$  and  $\beta = 0.5 \text{ km}^{-1}$ , and the initial inhomogeneity is characterized by peak plasma density  $2 \times 10^9 \text{ m}^{-3}$  and effective radius 30 m (Qin et al. 2012b). Reprinted by permission from American Geophysical Union

prediction advanced by Qin et al. (2013) that negative sprites (produced by -CGs) should necessarily be carrot sprites and most likely accompanied by a detectable halo, since the initiation of upward positive streamers is always easier than that of downward negative streamers, and -CGs are usually associated with impulsive return stroke with no continuing current.

### 3.7 Role of Electron Detachment in Sprites

Recent work indicates a possible importance of associative electron detachment processes for the initiation of long-delayed sprites (Luque and Gordillo-Vazquez 2012) and in definition of time dynamics of sprite halos (Liu 2012), in particular suggesting that additional downward progression of sprite halo due to the electron detachment may explain initiation of some sprites at altitudes as low as 65–70 km (Liu 2012). Luque and Gordillo-Vazquez (2012) emphasized that the associative detachment process is a fundamental process in upper-atmospheric electrodynamics. This process is important on timescales of 10s of milliseconds at sprite altitudes and allows electrons to multiply under electric field strengths significantly below the conventional breakdown field  $E_k$  (Luque and Gordillo-Vazquez 2012), where  $E_k$  is defined by equality of ionization and dissociative attachment coefficients in air, as introduced in Sect. 2.1.

The detachment process discussed above is represented by the reaction  $\text{O}^- + \text{N}_2 \rightarrow e + \text{N}_2\text{O}$  (Luque and Gordillo-Vazquez 2012; Liu 2012) and is a process by which electrons produced by ionization of  $\text{N}_2$  and  $\text{O}_2$  and removed by dissociative attachment  $e + \text{O}_2 \rightarrow \text{O} + \text{O}^-$  are returned back to free electron population. The timescale of electron multiplication when this process is taken into account therefore cannot be shorter than timescale of ionization. At typical sprite altitudes of  $\sim 75 \text{ km}$  and at fields 10 % below  $E_k$  the characteristic ionization timescale (i.e.,  $1/\nu_i$ , where  $\nu_i$  is the ionization frequency) is  $\simeq 0.5 \text{ ms}$ , which is a long timescale in comparison with typical timescales of growth of sprite streamers observed experimentally. The actual timescale is longer because the detachment process is not instantaneous and depends on the concentration of  $\text{O}^-$  ions. Quantitative analysis indicates that detachment process becomes pronounced on timescales of 10 s of milliseconds at typical sprite altitudes (Luque and Gordillo-Vazquez 2012; Liu 2012).

Liu (2012) performed accurate time dynamic modeling of sprite halos with inclusion of the electron detachment and noted that no pronounced electron attachment “hole” observed in previous halo studies was formed below the halo front. These results are in good agreement with earlier findings obtained using a similar electron detachment model by Neubert et al. (2011, Fig. 12b). Recent work of Marshall (2012) on the interaction of lightning electromagnetic pulses (EMPs) with the lower ionosphere also indicated that the detachment process reduces the ability of EMPs to deplete the lower ionospheric electron density. In this context, we also note that the most recent experimental evidence based on the measurements of subionospherically propagating VLF/LF electromagnetic waves does indicate significant (orders of magnitude) depletions in lower ionospheric electron density (Shao et al. 2013).

The results of Liu (2012) indicate that electron density can grow during the halo dynamics in regions of space where electric field never exceeds  $E_k$ . Liu (2012) explains growth of electron density in  $E < E_k$  when there are abundant  $O^-$  ions in space as follows. Electrons are still produced below the breakdown threshold field  $E_k$  due to electron impact ionization and they are constantly converted to  $O^-$  by the attachment process at the same time. Therefore, the total density of electrons and  $O^-$  ions increases as long as the ionization is effective (recombination takes place on a much longer timescale). When  $O^-$  ions accumulate to certain level, the detachment process becomes faster than the attachment process and then electron density increases together with the  $O^-$  density if significant ionization is continuously produced by the electron impact ionization (Liu 2012). Liu (2012) also points that detachment of electrons from  $O^-$  ions makes the photoionization process less important, because the detachment also can generate free electrons ahead of the halo front.

It is important to emphasize that in the context of initiation of sprite streamers (see Sect. 2.4), the electron avalanche cannot develop and transform into a streamer under  $E < E_k$  conditions (Liu 2012). Solutions of kinetic equations presented by Liu (2012) indicate that for initial conditions with zero density of  $O^-$  ions and nonzero electron density under  $E < E_k$  conditions, the initial dynamics of the system always shows reduction in electron density due to the predominance of the dissociative attachment (until significant number of  $O^-$  ions accumulates). For a small initial inhomogeneity (emulating an electron avalanche suddenly introduced in the region with  $E < E_k$ ) moving under the influence of electric field, the electrons dynamically shift to new regions of space free of  $O^-$  ions and therefore the density of electrons is expected to be dynamically reduced, as opposite to exponential growth in case when  $E > E_k$  (Liu 2012).

Pachter et al. (2012) recently investigated the role of electron detachment in inception of long-delayed sprites, specifically focusing on modification (i.e., lowering) of effective  $E_k$  values due to the detachment process following formulation of Luque and Gordillo-Vazquez (2012). Pachter et al. (2012) investigated the effective  $E_k$  as a function ratio of density of  $O^-$  ions to density of electrons and observed several percent reduction in  $E_k$  when the ratio varied from zero to 1. In the context of dynamical behavior of the system, Pachter et al. (2012) noted also that additional release of electrons due to detachment leading to increase in ambient conductivity led to a factor of four greater relative reduction in electric field due to relaxation in conducting medium. Pachter et al. (2012) therefore concluded that the detachment process is unfavorable for the initiation of long-delayed sprites as it reduces the magnitude of the electric field that otherwise would be available to drive electron avalanches from preexisting inhomogeneities into streamers.

### 3.8 Diagnostics of Electric Field in Streamers in Sprites and Other Transient Luminous Events

The electric fields associated with streamer discharges in TLEs are now routinely measured considering the ratios of spatially integrated radiation intensities of band systems with different energy excitation thresholds (e.g., Kuo et al. 2005; Liu et al. 2006; Adachi et al. 2006; Kuo et al. 2009; Liu et al. 2009b). In a streamer, the head is usually responsible for the most part of ionization and excitation of species and therefore is responsible for the most part of emissions. However, the spatial nonuniformity of streamer discharges is such that the maximum excitation rates are not exactly located at the spatial position of the maximum electric field (Naidis 2009). Following recent work by Naidis (2009), Celestin and Pasko (2010) demonstrated that, due to strong spatial variations of the electron density and electric field in streamer heads, previous measurements may lead to a significant underestimation of the peak values of electric fields in TLEs. The modeling analysis of streamers, as a function of altitude, applied reduced electric field, and streamer polarity conducted by Celestin and Pasko (2010) indicated that the ratio-based electric fields derived from spectrophotometric data need to be multiplied by a corrective factor  $>1.4$  for positive streamers and  $>1.5$  for negative streamers, to obtain the true peak values of electric fields.

The study of Celestin and Pasko (2010) brings the values of electric field previously deduced from observations (e.g., Kuo et al. 2005; Adachi et al. 2006) much closer to streamer simulations. Moreover, one can note that the value  $5.5E_k$  documented in (Kuo et al. 2009) for negative gigantic jet discharge would lead to the very high field  $>1.5 \times 5.5E_k \simeq 8E_k$  approaching or exceeding magnitudes for which thermal electron runaway process becomes possible (e.g., Moss et al. 2006; Li et al. 2009; Chanrion and Neubert 2008, 2010; Celestin and Pasko 2011). These results, therefore, have direct implications for the production of runaway electrons in jet discharges. We note that these electric field magnitudes are significantly greater than those observed in early sprite studies ( $\sim E_k$ ) (Morrill et al. 2002, and references therein), and the difference can be explained by low temporal resolution of their observations (Liu and Pasko 2005).

### 3.9 Conductivity Perturbations Associated with Sprites

Recent results reported by Haldoupis et al. (2010) once again reiterate an important point made in previous sections that some sprites may remain subvisual in spite of their initiation and significant conductivity perturbations they produce in the lower ionosphere. Haldoupis et al. (2010) reported narrowband VLF observations in which multiple transmitter–receiver VLF pairs with great circle paths passing near a sprite-producing thunderstorm were available and presented an evidence that visible sprite occurrences are accompanied by early VLF perturbations in a one-to-one correspondence. The early VLF events are abrupt perturbations of subionospherically propagating VLF waves (including both perturbations in amplitude and phase) that occur within 20 ms of a lightning event. The observations of Haldoupis et al. (2010) imply that the sprite generation mechanism may cause also subionospheric conductivity disturbances that produce early VLF events. However, the one-to-one visible sprite to early VLF event correspondence, if viewed conversely, appears not to be always reciprocal (Haldoupis et al. 2010). This is because the number of early events detected in some case studies was considerably larger than the number of visible sprites. Since the great majority of the early events not accompanied by visible sprites appeared to be caused by positive cloud-to-ground (+CG) lightning discharges, it is possible that

sprites or sprite halos were concurrently present in these events as well but were missed by the sprite-watch camera detection system (Haldoupis et al. 2010). More recent work of Haldoupis et al. (2012) indicates that lower ionospheric modifications caused by intense +CGs can last up to 30 min. In terms of general discussion of conductivity/chemical perturbations associated with sprites, the average conductivity in the sprite volume deduced from ELF radiation emitted by sprite current is  $\sim 10^{-7}$  S/m (Pasko et al. 1998b). A recent study of Gordillo-Vazquez and Luque (2010) indicates that larger conductivity changes are possible due to associative detachment of electrons from  $O^-$  ions in the trailing regions of long sprite streamers when electric field in these regions approaches the conventional breakdown threshold field during the later stages of sprite evolution (see related discussion of (Liu 2010) and (Luque and Ebert 2010) in Sect. 3.3, and also discussion about other effects of electron detachment in Sect. 3.7).

#### 4 Summary

In this review, we presented a brief overview of basic physical mechanisms and parameters needed for understanding of sprite phenomenology, followed by a survey of recent literature relevant to initiation, morphology, and polarity asymmetry of sprite streamers. Sprite mechanisms based on the penetration of quasi-static electric field to mesospheric/lower ionospheric altitudes are described and the lightning charge moment change is introduced as an important parameter that allows to quantify lightning potential to create sprites. It is emphasized that a large charge moment change is a necessary but not sufficient condition for the creation of sprites with well-developed streamer structures. Reasons for conversion of sprite luminosity from diffuse form at high altitudes to more structured forms at lower altitudes are presented, followed by a brief summary discussion of critical fields required for the propagation of streamers of positive and negative polarity and similarity relations allowing to scale properties of streamers as a function of air density. The importance of inhomogeneities is emphasized and basic processes involved in avalanche-to-streamer transition are then reviewed. The acceleration, expansion, and exponential growth of brightness of streamers propagating in fields exceeding minimum fields required for the propagation of positive and negative streamers are introduced as important properties of streamers in sprites observed experimentally.

This discussion is followed by overview of conditions of initiation of positive and negative streamers in sprites from preexisting plasma inhomogeneities. Recent literature targeting understanding of afterglow region in sprite streamers and dependence of initiation of sprite streamers on vertical elongation of plasma inhomogeneities is then discussed. The exact conditions leading to the initiation of columniform and carrot sprites that are linked to conditions of initiation of single- and double-headed streamers, respectively, are presented. A sprite polarity paradox is reviewed and emphasis is placed on the physics of streamers and their observability as critical factors contributing to extremely rare occurrences of observable negative sprites. The minimum charge moment changes required for the initiation of sprites of negative and positive polarity are discussed, followed by the analysis of effects of electron detachment on sprite initiation and dynamics. The maximum electric fields that can exist in streamers in sprites and in other types of transient luminous events are reviewed along with remote sensing techniques used for their detection. The large-scale conductivity perturbations associated with sprites are discussed, emphasizing that in spite of the significant conductivity changes, many sprites remain subvisual and are missed during optical observations.

**Acknowledgments** This research was supported by the United States National Science Foundation under AGS-0734083 Grant to Penn State University. S. Celestin's research is supported by the French Space Agency (CNES).

## References

- Achat S, Teisseyre Y, Marode E (1992) The scaling of the streamer-to-arc transition in a positive point-to-plane gap with pressure. *J Phys D Appl Phys* 25(4):661–668
- Adachi T, Fukunishi H, Takahashi Y, Hiraki Y, Hsu RR, Su HT, Chen AB, Mende SB, Frey HU, Lee LC (2006) Electric field transition between the diffuse and streamer regions of sprites estimated from ISUAL/array photometer measurements. *Geophys Res Lett* 33(17):L17803
- Allen NL, Ghaffar A (1995) The conditions required for the propagation of a cathode-directed positive streamer in air. *J Phys D Appl Phys* 28:331–337
- Babaeva NY, Naidis GV (1997) Dynamics of positive and negative streamers in air in weak uniform electric fields. *IEEE Trans Plasma Sci* 25:375–379
- Barrington-Leigh CP, Inan US, Stanley M (2001) Identification of sprites and elves with intensified video and broadband array photometry. *J Geophys Res* 106(A2):1741–1750. doi:10.1029/2000JA000073
- Bazelyan EM, Raizer YP (2000) *Lightning physics and lightning protection*, IoP Publishing Ltd, Bristol
- Boeck WL, Vaughan OH, Blakeslee RJ, Vonnegut B, Brook M (1998) The role of the space shuttle videotapes in the discovery of sprites, jets and elves. *J Atmos Sol Terr Phys* 60:669–677
- Bourdon A, Pasko VP, Liu NY, Celestin S, Segur P, Marode E (2007) Efficient models for photoionization produced by non-thermal gas discharges in air based on radiative transfer and the Helmholtz equations. *Plasma Source Sci Technol* 16:656–678
- Briels TMP, Kos J, van Veldhuizen EM, Ebert U (2006) Circuit dependence of the diameter of pulsed positive streamers in air. *J Phys D Appl Phys* 39:5201–5210
- Bucselu E, Morrill J, Heavner M, Siefing C, Berg S, Hampton D, Moudry D, Wescott E, Sentman D (2003)  $N_2(B^3\Pi_g)$  and  $N_2^+(A^2\Pi_u)$  vibrational distributions observed in sprites. *J Atmos Sol Terr Phys* 65:583–590
- Celestin S, Pasko VP (2010) Effects of spatial non-uniformity of streamer discharges on spectroscopic diagnostics of peak electric fields in transient luminous events. *Geophys Res Lett* 37:L07804
- Celestin S, Pasko VP (2011) Energy and fluxes of thermal runaway electrons produced by exponential growth of streamers during the stepping of lightning leaders and in transient luminous events. *J Geophys Res* 116:A03315
- Chanrion O, Neubert T (2008) A PIC-MCC code for simulation of streamer propagation in air. *J Comput Phys* 227(15):7222–7245
- Chanrion O, Neubert T (2010) Production of runaway electrons by negative streamer discharges. *J Geophys Res* 115:A00E32. doi:10.1029/2009JA014774
- Cummer SA, Lyons WA (2005) Implication of lightning charge moment changes for sprite initiation. *J Geophys Res* 110:A04304. doi:10.1029/2004JA010812
- Cummer SA, Jaugey NC, Li JB, Lyons WA, Nelson TE, Gerken EA (2006) Submillisecond imaging of sprite development and structure. *Geophys Res Lett* 33:L04104. doi:10.1029/2005GL024969
- Dhali SK, Williams PF (1987) Two-dimensional studies of streamers in gases. *J Appl Phys* 62:4696–4707
- Ebert U, Sentman D (2008) Editorial Review: Streamers, sprites, leaders, lightning: from micro- to macroscales. *J Phys D Appl Phys* 41:230301
- Ebert U, Nijdam S, Li C, Luque A, Briels T, van Veldhuizen E (2010) Review of recent results on streamer discharges and discussion of their relevance for sprites and lightning. *J Geophys Res* 115:A00E43
- Fishman GJ, Bhat PN, Mallozzi R, Horack JM, Koshut T, Kouveliotou C, Pendleton GN, Meegan CA, Wilson RB, Paciesas WS, Goodman SJ, Christian HJ (1994) Discovery of intense gamma-ray flashes of atmospheric origin. *Science* 264(5163):1313–1316
- Frey HU, Mende SB, Cummer SA, Li J, Adachi T, Fukunishi H, Takahashi Y, Chen AB, Hsu RR, Su HT, Chang YS (2007) Halos generated by negative cloud-to-ground lightning. *Geophys Res Lett* 34:L18801
- Gallimberti I, Bacchiega G, Bondiou-Clergerie A, Lalande P (2002) Fundamental processes in long air gap discharges. *C R Phys* 3(10):1335–1359. doi:10.1016/S1631-0705(02)01414-7
- Gerken EA, Inan US (2002) A survey of streamer and diffuse glow dynamics observed in sprites using telescopic imagery. *J Geophys Res* 107(A11):1344. doi:10.1029/2002JA009248
- Gerken EA, Inan US (2003) Observations of decameter-scale morphologies in sprites. *J Atmos Sol Terr Phys* 65:567–572. doi:10.1016/S1364-6826(02)00333-4

- Gerken EA, Inan US, Barrington-Leigh CP (2000) Telescopic imaging of sprites. *Geophys Res Lett* 27:2637–2640
- Gordillo-Vazquez FJ, Luque A (2010) Electrical conductivity in sprite streamer channels. *Geophys Res Lett* 37:L16809. doi:[10.1029/2010GL044349](https://doi.org/10.1029/2010GL044349)
- Haldoupis C, Amvrosiadi N, Cotts BRT, van der Velde OA, Chanrion O, Neubert T (2010) More evidence for a one-to-one correlation between Sprites and Early VLF perturbations. *J Geophys Res* 115:A07304
- Haldoupis C, Cohen M, Cotts B, Arnone E, Inan U (2012) Long-lasting D-region ionospheric modifications, caused by intense lightning in association with elve and sprite pairs. *Geophys Res Lett* 39:L16801
- Han F, Cummer SA (2010) Midlatitude nighttime D region ionosphere variability on hourly to monthly time scales. *J Geophys Res* 115:A09323. doi:[10.1029/2010JA015437](https://doi.org/10.1029/2010JA015437)
- Hayakawa M, Nakamura T, Hobara Y, Williams E (2004) Observation of sprites over the Sea of Japan and conditions for lightning-induced sprites in winter. *J Geophys Res* 109:A01312. doi:[10.1029/2003JA009905](https://doi.org/10.1029/2003JA009905)
- Hu WY, Cummer SA, Lyons WA (2002) Lightning charge moment changes for the initiation of sprites. *Geophys Res Lett* 29(8):1279. doi:[10.1029/2001GL014593](https://doi.org/10.1029/2001GL014593)
- Hu WY, Cummer SA, Lyons WA (2007) Testing sprite initiation theory using lightning measurements and modeled electromagnetic fields. *J Geophys Res* 112(D13):D13115
- Inan US (2002) Lightning effects at high altitudes: sprites, elves, and terrestrial gamma ray flashes. *C R Phys* 3(10):1411–1421
- Inan US, Cummer SA, Marshall RA (2010) A survey of ELF and VLF research on lightning-ionosphere interactions and causative discharges. *J Geophys Res* 115:A00E36
- Kanmae T, Stenbaek-Nielsen HC, McHarg MG (2007) Altitude resolved sprite spectra with 3 ms temporal resolution. *Geophys Res Lett* 34:L07810
- Kanmae T, Stenbaek-Nielsen HC, McHarg MG, Haaland RK (2012) Diameter–speed relation of sprite streamers. *J Phys D Appl Phys* 45(27):275203. doi:[10.1088/0022-3727/45/27/275203](https://doi.org/10.1088/0022-3727/45/27/275203)
- Kosar BC, Liu NY, Rassoul HK (2012) Luminosity and propagation characteristics of sprite streamers initiated from small ionospheric disturbances at sub-breakdown conditions. *J Geophys Res* 117:A08328. doi:[10.1029/2012JA017632](https://doi.org/10.1029/2012JA017632)
- Kuo CL (2012) The middle atmosphere: discharge phenomena. In: Ghadawala R (ed) *Advances in spacecraft systems and orbit determination*, InTech, Shanghai, pp 1–28
- Kuo CL, Hsu RR, Su HT, Chen AB, Lee LC, Mende SB, Frey HU, Fukunishi H, Takahashi Y (2005) Electric fields and electron energies inferred from the ISUAL recorded sprites. *Geophys Res Lett* 32:L19103. doi:[10.1029/2005GL023389](https://doi.org/10.1029/2005GL023389)
- Kuo CL, Chou JK, Tsai LY, Chen AB, Su HT, Hsu RR, Cummer SA, Frey HU, Mende SB, Takahashi Y, Lee LC (2009) Discharge processes, electric field, and electron energy in ISUAL-recorded gigantic jets. *J Geophys Res* 114:A04314
- Lang TJ, Li J, Lyons WA, Cummer SA, Rutledge SA, MacGorman DR (2011) Transient luminous events above two mesoscale convective systems: charge moment change analysis. *J Geophys Res* 116:A10306. doi:[10.1029/2011JA016758](https://doi.org/10.1029/2011JA016758)
- Li C, Ebert U, Hundsdorfer W (2009) 3D hybrid computations for streamer discharges and production of runaway electrons. *J Phys D Appl Phys* 42(20):202003. doi:[10.1088/0022-3727/42/20/202003](https://doi.org/10.1088/0022-3727/42/20/202003)
- Li J, Cummer S (2011) Estimation of electric charge in sprites from optical and radio observations. *J Geophys Res* 116:A01301. doi:[10.1029/2010JA015391](https://doi.org/10.1029/2010JA015391)
- Li J, Cummer SA (2009) Measurement of sprite streamer acceleration and deceleration. *Geophys Res Lett* 36:L10812
- Li J, Cummer SA (2012) Relationship between sprite streamer behavior and lightning-driven electric fields. *J Geophys Res* 117:A01317
- Li J, Cummer SA, Lu G, Zigoneanu L (2012) Charge moment change and lightning-driven electric fields associated with negative sprites and halos. *J Geophys Res* 117:A09310. doi:[10.1029/2012JA017731](https://doi.org/10.1029/2012JA017731)
- Liu NY (2010) Model of sprite luminous trail caused by increasing streamer current. *Geophys Res Lett* 37:L04102. doi:[10.1029/2009GL042214](https://doi.org/10.1029/2009GL042214)
- Liu NY (2012) Multiple ion species fluid modeling of sprite halos and the role of electron detachment of  $O^-$  in their dynamics. *J. Geophys. Res.* 117:A03308. doi:[10.1029/2011JA017062](https://doi.org/10.1029/2011JA017062)
- Liu NY, Pasko VP (2004) Effects of photoionization on propagation and branching of positive and negative streamers in sprites. *J Geophys Res* 109:A04301. doi:[10.1029/2003JA010064](https://doi.org/10.1029/2003JA010064)
- Liu NY, Pasko VP (2005) Molecular nitrogen LBH band system far-UV emissions of sprite streamers. *Geophys Res Lett* 32:L05104. doi:[10.1029/2004GL022001](https://doi.org/10.1029/2004GL022001)
- Liu NY, Pasko VP (2006) Effects of photoionization on similarity properties of streamers at various pressures in air. *J Phys D Appl Phys* 39:327–334. doi:[10.1088/0022-3727/39/2/013](https://doi.org/10.1088/0022-3727/39/2/013)
- Liu NY, Pasko VP (2010) NO-gamma emissions from streamer discharges: direct electron impact excitation versus resonant energy transfer. *J Phys D Appl Phys* 43:082001

- Liu NY, Pasko VP, Burkhardt DH, Frey HU, Mende SB, Su H-T, Chen AB, Hsu R-R, Lee L-C, Fukunishi H, Takahashi Y (2006) Comparison of results from sprite streamer modeling with spectrophotometric measurements by ISUAL instrument on FORMOSAT-2 satellite. *Geophys Res Lett* 33:L01101. doi:[10.1029/2005GL024243](https://doi.org/10.1029/2005GL024243)
- Liu NY, Pasko VP, Adams K, Stenbaek-Nielsen HC, McHarg MG (2009) Comparison of acceleration, expansion, and brightness of sprite streamers obtained from modeling and high-speed video observations. *J Geophys Res* 114:A00E03
- Liu NY, Pasko VP, Frey HU, Mende SB, Su H-T, Chen AB, Hsu R-R, Lee L-C (2009) Assessment of sprite initiating electric fields and quenching altitude of a  $^1\Pi_g$  state of  $N_2$  using sprite streamer modeling and ISUAL spectrophotometric measurements. *J Geophys Res* 114:A00E02
- Liu NY, Kosar B, Sadighi S, Dwyer JR, Rassoul HK (2012) Formation of streamer discharges from an isolated ionization column at subbreakdown conditions. *Phys Rev Lett* 109(2):025002. doi:[10.1103/PhysRevLett.109.025002](https://doi.org/10.1103/PhysRevLett.109.025002)
- Loeb LB, Meek JM (1940) The mechanism of spark discharge in air at atmospheric pressure. *J Appl Phys* 11:438–447
- Lu G, Blakeslee RJ, Li J, Smith DM, Shao XM, McCaul EW, Buechler DE, Christian HJ, Hall JM, Cummer SA (2010) Lightning mapping observation of a terrestrial gamma-ray flash. *Geophys Res Lett* 37:L11806. doi:[10.1029/2010GL043494](https://doi.org/10.1029/2010GL043494)
- Lu G, Cummer SA, Li J, Han F, Smith DM, Grefenstette BW (2011) Characteristics of broadband lightning emissions associated with terrestrial gamma ray flashes. *J Geophys Res* 116:A03316. doi:[10.1029/2010JA016141](https://doi.org/10.1029/2010JA016141)
- Lu G, Cummer SA, Blakeslee RJ, Weiss S, Beasley WH (2012) Lightning morphology and impulse charge moment change of high peak current negative strokes. *J Geophys Res* 117:D04212. doi:[10.1029/2011JD016890](https://doi.org/10.1029/2011JD016890)
- Luque A, Ebert U (2009) Emergence of sprite streamers from screening-ionization waves in the lower ionosphere. *Nat Geosci* 2(11):757–760. doi:[10.1038/NGEO662](https://doi.org/10.1038/NGEO662)
- Luque A, Ebert U (2010) Sprites in varying air density: charge conservation, glowing negative trails and changing velocity. *Geophys Res Lett* 37:L06806. doi:[10.1029/2009GL041982](https://doi.org/10.1029/2009GL041982)
- Luque A, Gordillo-Vazquez FJ (2011) Sprite beads originating from inhomogeneities in the mesospheric electron density. *Geophys Res Lett* 38:L04808. doi:[10.1029/2010GL046403](https://doi.org/10.1029/2010GL046403)
- Luque A, Gordillo-Vazquez FJ (2012) Mesospheric electric breakdown and delayed sprite ignition caused by electron detachment. *Nat Geosci* 5(1):22–25. doi:[10.1038/NGEO1314](https://doi.org/10.1038/NGEO1314)
- Lyons WA (1996) Sprite observations above the U.S. high plains in relation to their parent thunderstorm systems. *J Geophys Res* 101:29,641–29, 652
- Lyons WA, Nelson TE, Armstrong RA, Pasko VP, Stanley MA (2003) Upward electrical discharges from thunderstorm tops. *Bull Am Meteorol Soc* 84(4):445–454. doi:[10.1175/BAMS-84-4-445](https://doi.org/10.1175/BAMS-84-4-445)
- Marshall RA (2012) An improved model of the lightning electromagnetic field interaction with the D-region ionosphere. *J Geophys Res* 117:A03316
- Marshall RA, Inan US (2006) High-speed measurements of small-scale features in sprites: Sizes and lifetimes. *Radio Sci* 41:RS6S43. doi:[10.1029/2005RS003353](https://doi.org/10.1029/2005RS003353)
- Marshall TC, Rust WD (1993) Two types of vertical electrical structures in stratiform precipitation regions of mesoscale convective systems. *Bull Am Meteorol Soc* 74(11):2159–2170
- McHarg MG, Stenbaek-Nielsen HC, Kanmae T (2007) Streamer development in sprites. *Geophys Res Lett* 34:L06804. doi:[10.1029/2006GL027854](https://doi.org/10.1029/2006GL027854)
- McHarg MG, Stenbaek-Nielsen HC, Kanmae T, Haaland RK (2010) Streamer tip splitting in sprites. *J Geophys Res* 115:A00E53. doi:[10.1029/2009JA014850](https://doi.org/10.1029/2009JA014850)
- McHarg MG, Stenbaek-Nielsen HC, Kanmae T, Haaland RK (2011) High-speed imaging of sprite streamers. *IEEE Trans Plasma Sci* 39(11, Part 1, SI):2266–2267. doi:[10.1109/TPS.2011.2165299](https://doi.org/10.1109/TPS.2011.2165299)
- Meek J (1940) A theory of spark discharge. *Phys Rev* 57(8):722–728
- Mishin EV, Milikh GM (2008) Blue jets: upward lightning. *Space Sci Rev* 137(1–4):473–488
- Montijn C, Ebert U (2006) Diffusion correction to the Raether–Meek criterion for the avalanche-to-streamer transition. *J Phys D Appl Phys* 39(14):2979–2992. doi:[10.1088/0022-3727/39/14/017](https://doi.org/10.1088/0022-3727/39/14/017)
- Morrill J, Bucsela E, Siefiring C, Heavner M, Berg S, Moudry D, Slinker S, Fernsler R, Wescott E, Sentman D, Osborne D (2002) Electron energy and electric field estimates in sprites derived from ionized and neutral  $N_2$  emissions. *Geophys Res Lett* 29(10):1462. doi:[10.1029/2001GL014018](https://doi.org/10.1029/2001GL014018)
- Morrill JS, Bucsela EJ, Pasko VP, Berg SL, Benesch WM, Wescott EM, Heavner MJ (1998) Time resolved  $N_2$  triplet state vibrational populations and emissions associated with red sprites. *J Atmos Sol Terr Phys* 60:811–829
- Morrow R, Lowke JJ (1997) Streamer propagation in air. *J Phys D Appl Phys* 30:614–627

- Moss GD, Pasko VP, Liu NY, Veronis G (2006) Monte Carlo model for analysis of thermal runaway electrons in streamer tips in transient luminous events and streamer zones of lightning leaders. *J Geophys Res* 111:A02307. doi:[10.1029/2005JA011350](https://doi.org/10.1029/2005JA011350)
- Naidis GV (2009) Positive and negative streamers in air: velocity–diameter relation. *Phys Rev E* 79(5, Part 2):057401. doi:[10.1103/PhysRevE.79.057401](https://doi.org/10.1103/PhysRevE.79.057401)
- Neubert T, Rycroft M, Farges T, Blanc E, Chanrion O, Arnone E, Odzimek A, Arnold N, CF CFE, Turunen E, Bosinger T, Mika A, Haldoupis C, Steiner RJ, van der Velde O, Soula O, Berg P, Boberg F, Thejll P, Christiansen B, Ignaccolo M, Fullekrug M, Verronen PT, Montanya J, Crosby N (2008) Recent results from studies of electric discharges in the mesosphere. *Surv Geophys* 29(2):71–137
- Neubert T, Chanrion O, Arnone E, Zanotti F, Cummer S, Li J, Fuellekrug M, Soula S, van der Velde O (2011) The properties of a gigantic jet reflected in a simultaneous sprite: observations interpreted by a model. *J Geophys Res* 116:A12329. doi:[10.1029/2011JA016928](https://doi.org/10.1029/2011JA016928)
- Pachter J, Qin J, Pasko VP (2012) Investigation of long-delayed sprite inception mechanism and the role of electron detachment. *NSF EE REU Penn State Annu Res J* 10:1–12
- Pasko VP (2006) Theoretical modeling of sprites and jets. In: Füllekrug M, Mareev EA, Rycroft MJ (eds) *Sprites, elves and intense lightning discharges*, NATO science series II: mathematics, physics and chemistry, 225th edn. Springer, Heidelberg, pp 253–311
- Pasko VP (2007) Red sprite discharges in the atmosphere at high altitude: the molecular physics and the similarity with laboratory discharges. *Plasma Sources Sci Technol* 16:S13–S29. doi:[10.1088/0963-0252/16/1/S02](https://doi.org/10.1088/0963-0252/16/1/S02)
- Pasko VP (2008) Blue jets and gigantic jets: transient luminous events between thunderstorm tops and the lower ionosphere. *Plasma Phys Control. Fusion* 50:124050
- Pasko VP (2010) Recent advances in theory of transient luminous events. *J Geophys Res* 50:A00E35
- Pasko VP, Stenbaek-Nielsen HC (2002) Diffuse and streamer regions of sprites. *Geophys Res Lett* 29(10):1440. doi:[10.1029/2001GL014241](https://doi.org/10.1029/2001GL014241)
- Pasko VP, Inan US, Bell TF (1995) Heating, ionization and upward discharges in the mesosphere due to intense quasi-electrostatic thundercloud fields. *Geophys Res Lett* 22(4):365–368
- Pasko VP, Inan US, Bell TF, Taranenko YN (1997) Sprites produced by quasi-electrostatic heating and ionization in the lower ionosphere. *J Geophys Res* 102(A3):4529–4561. doi:[10.1029/96JA03528](https://doi.org/10.1029/96JA03528)
- Pasko VP, Inan US, Bell TF (1998) Spatial structure of sprites. *Geophys Res Lett* 25:2123–2126
- Pasko VP, Inan US, Bell TF, Reising SC (1998) Mechanism of ELF radiation from sprites. *Geophys Res Lett* 25(18):3493–3496
- Pasko VP, Inan US, Bell TF (1999) Mesospheric electric field transients due to tropospheric lightning discharges. *Geophys Res Lett* 26:1247–1250
- Pasko VP, Inan US, Bell TF (2000) Fractal structure of sprites. *Geophys Res Lett* 27(4):497–500. doi:[10.1029/1999GL010749](https://doi.org/10.1029/1999GL010749)
- Pasko VP, Inan US, Bell TF (1996) Sprites as luminous columns of ionization produced by quasi-electrostatic thundercloud fields. *Geophys Res Lett* 23(6):649–652
- Pasko VP, Yair Y, Kuo C-L (2012) Lightning related transient luminous events at high altitude in the Earth's atmosphere: phenomenology, mechanisms and effects. *Space Sci Rev* 168(1–4):475–516. doi:[10.1007/s11214-011-9813-9](https://doi.org/10.1007/s11214-011-9813-9)
- Petrova NI, Petrova GN (1999) Physical mechanisms for the development of lightning discharges between a thundercloud and the ionosphere. *Tech Phys* 44:472–475
- Qin J, Celestin S, Pasko VP (2011) On the inception of streamers from sprite halo events produced by lightning discharges with positive and negative polarity. *J Geophys Res* 116:A06305
- Qin J, Celestin S, Pasko VP (2012) Formation of single and double-headed streamers in sprite-halo events. *Geophys Res Lett* 39:L05810. doi:[10.1029/2012GL051088](https://doi.org/10.1029/2012GL051088)
- Qin J, Celestin S, Pasko VP (2012) Minimum charge moment change in positive and negative cloud to ground lightning discharges producing sprites. *Geophys Res Lett* 39:L22801. doi:[2012GL053951](https://doi.org/10.1029/2012GL053951)
- Qin J, Celestin S, Pasko VP (2012) Low frequency electromagnetic radiation from sprite streamers. *Geophys Res Lett* 39:L22803. doi:[2012GL053991](https://doi.org/10.1029/2012GL053991)
- Qin J, Celestin S, Pasko VP (2013) Dependence of positive and negative sprite morphology on lightning characteristics and upper atmospheric ambient conditions. *J Geophys Res* 118:2623–2638. doi:[10.1029/2012JA017908](https://doi.org/10.1029/2012JA017908)
- Raizer YP (1991) *Gas discharge physics*, 225th edn, Springer, New York, NY
- Raizer YP, Milikh GM, Shneider MN, Novakovski SV (1998) Long streamers in the upper atmosphere above thundercloud. *J Phys D Appl Phys* 31:3255–3264
- Raizer YP, Milikh GM, Shneider MN (2010) Streamer- and leader-like processes in the upper atmosphere: models of red sprites and blue jets. *J Geophys Res* 115:A00E42

- Rocco A, Ebert U, Hundsdoerfer W (2002) Branching of negative streamers in free flight. *Phys Rev E* 66:035102(R). doi:[10.1103/PhysRevE.66.035102](https://doi.org/10.1103/PhysRevE.66.035102)
- Rodger CJ (1999) Red sprites, upward lightning and VLF perturbations. *Rev Geophys* 37:317–336
- Roth RJ (1995) Industrial plasma engineering, vol 1: principles, IOP Publishing Ltd, Bristol
- Roussel-Dupre R, Colman JJ, Symbalisty E, Sentman D, Pasko VP (2008) Physical processes related to discharges in planetary atmospheres. *Space Sci Rev* 137(1–4):51–82
- Sentman DD, Stenbaek-Nielsen HC (2009) Chemical effects of weak electric fields in the trailing columns of sprite streamers. *Plasma Sources Sci Technol* 18(3):034012
- Sentman DD, Wescott EM, Osborne DL, Hampton DL, Heavner MJ (1995) Preliminary results from the Sprites94 campaign: red sprites. *Geophys Res Lett* 22:1205–1208
- Sentman DD, Stenbaek-Nielsen HC, McHarg MG, Morrill JS (2008) Plasma chemistry of sprite streamers. *J Geophys Res* 113:D11112
- Shao X-M, Lay EH, Jacobson AR (2013) Reduction of electron density in the night-time lower ionosphere in response to a thunderstorm. *Nat Geosci* 6(1):29–33. doi:[10.1038/NNGEO1668](https://doi.org/10.1038/NNGEO1668)
- Shepherd TR, Rust WD, Marshall TC (1996) Electric fields and charges near 0 degrees C in stratiform clouds. *Mon Weather Rev* 124(5):919–938
- Siingh D, Singh AK, Patel RP, Singh R, Singh RP, Veenadhari B, Mukherjee M (2008) Thunderstorms, lightning, sprites and magnetospheric whistler-mode radio waves. *Surv Geophys* 29(6):499–551
- Smith DM, Lopez LI, Lin RP, Barrington-Leigh CP (2005) Terrestrial gamma-ray flashes observed up to 20 MeV. *Science* 307(5712):1085–1088. doi:[10.1126/science.1107466](https://doi.org/10.1126/science.1107466)
- Stanley M, Krehbiel P, Brook M, Moore C, Rison W, Abrahams B (1999) High speed video of initial sprite development. *Geophys Res Lett* 26:3201–3204
- Stenbaek-Nielsen HC, McHarg MG (2008) High time-resolution sprite imaging: observations and implications. *J Phys D Appl Phys* 41:234009
- Stenbaek-Nielsen HC, Moudry DR, Wescott EM, Sentman DD, Sabbas FTS (2000) Sprites and possible mesospheric effects. *Geophys Res Lett* 27:3829–3832
- Stenbaek-Nielsen HC, McHarg MG, Kanmae T, Sentman DD (2007) Observed emission rates in sprite streamer heads. *Geophys Res Lett* 34:L11105. doi:[10.1029/2007GL029881](https://doi.org/10.1029/2007GL029881)
- Stenbaek-Nielsen HC, Kanmae T, McHarg MG, Haaland R (2013) High speed observations of sprite streamers. *Surv Geophys*. doi:[10.1007/s10712-013-9224-4](https://doi.org/10.1007/s10712-013-9224-4)
- Stenbaek-Nielsen HC, Haaland R, McHarg MG, Hensley BA, Kanmae T (2010) Sprite initiation altitude measured by triangulation. *J Geophys Res* 115:A00E12. doi:[10.1029/2009JA014543](https://doi.org/10.1029/2009JA014543)
- Surkov VV, Hayakawa M (2012) Underlying mechanisms of transient luminous events: a review. *Ann Geophys Atmos Hydrospheres Space Sci* 30(8):1185–1212. doi:[10.5194/angeo-30-1185-2012](https://doi.org/10.5194/angeo-30-1185-2012)
- Tardiveau P, Marode E, Agneray A, Cheaib M (2001) Pressure effects on the development of an electric discharge in non-uniform fields. *J Phys D Appl Phys* 34:1690–1696
- Tavani M, Marisaldi M, Labanti C, Fuschino F, Argan A, Trois A, Giommi P, Colafrancesco S, Pittori C, Palma F, Trifoglio M, Gianotti F, Bulgarelli A, Vittorini V, Verrecchia F, Salotti L, Barbiellini G, Caraveo P, Cattaneo PW, Chen A, Contessi T, Costa E, D'Ammando F, Del Monte E, De Paris G, Di Cocco G, Di Persio G, Donnarumma I, Evangelista Y, Feroci M, Ferrari A, Galli M, Giuliani A, Giusti M, Lapshov I, Lazzarotto F, Lipari P, Longo F, Mereghetti S, Morelli E, Moretti E, Morselli A, Pacciani L, Pellizzoni A, Perotti F, Piano G, Picozza P, Pilia M, Pucella G, Prest M, Rapisarda M, Rappoldi A, Rossi E, Rubini A, Sabatini S, Scalise E, Soffitta P, Striani E, Vallazza E, Vercellone S, Zambra A, Zanello D, AGILE Team (2011) Terrestrial gamma-ray flashes as powerful particle accelerators. *Phys Rev Lett* 106(1):018501. doi:[10.1103/PhysRevLett.106.018501](https://doi.org/10.1103/PhysRevLett.106.018501)
- Vadislavsky E, Yair Y, Erlick C, Price C, Greenberg E, Yaniv R, Ziv B, Reicher N, Devir A (2009) Indication for circular organization of column sprite elements associated with Eastern Mediterranean winter thunderstorms. *J Atmos Sol Terr Phys* 71(17–18):1835–1839. doi:[10.1016/j.jastp.2009.07.001](https://doi.org/10.1016/j.jastp.2009.07.001)
- Veronis G, Pasko VP, Inan US (2001) Characteristics of mesospheric optical emissions produced by lightning discharges. *J Geophys Res* 104(A6):12645–12656
- Vitello PA, Penetrante BM, Bardsley JN (1993) Multidimensional modeling of the dynamic morphology of streamer coronas. In: Penetrante BM, Schultheis SE (eds) Non-thermal plasma techniques for pollution control, NATO ASI Series. G34, part A edn. Springer, New York, pp 249–271
- Vitello PA, Penetrante BM, Bardsley JN (1994) Simulation of negative-streamer dynamics in nitrogen. *Phys Rev E* 49:5574–5598
- Wait JR, Spies KP (1964) Characteristics of the Earth-ionosphere waveguide for VLF radio waves, Tech note 300, National Bureau of Standards, Boulder, CO
- Williams E, Downes E, Boldi R, Lyons W, Heckman S (2007) Polarity asymmetry of sprite-producing lightning: a paradox? *Radio Sci* 42:RS2S17. doi:[10.1029/2006RS003488](https://doi.org/10.1029/2006RS003488)

- Williams E, Kuo CL, Bor J, Satori G, Newsome R, Adachi T, Boldi R, Chen A, Downes E, Hsu RR, Lyons W, Saba MMF, Taylor M, Su HT (2012) Resolution of the sprite polarity paradox: the role of halos. *Radio Sci* 47:RS2002. doi:[10.1029/2011RS004794](https://doi.org/10.1029/2011RS004794)
- Wilson CTR (1925) The electric field of a thundercloud and some of its effects. *Proc Phys Soc Lond* 37:32D–37D
- Zabotin NA, Wright JW (2001) Role of meteoric dust in sprite formation. *Geophys Res Lett* 28(13):2593–2596. doi:[10.1029/2000GL012699](https://doi.org/10.1029/2000GL012699)